

Extreme events in solutions of hydrostatic and non-hydrostatic climate models

J. D. Gibbon and Darryl D. Holm

Department of Mathematics, Imperial College London, London SW7 2AZ, UK

October 22, 2021

Contents

1	General Introduction	3
1.1	Introductory remarks	3
1.2	Hydrostatic primitive equations (HPE)	8
1.3	Non-hydrostatic primitive equations (NPE)	9
2	The main results & their interpretation	10
2.1	Results in the hydrostatic case (HPE)	10
2.2	Results in the non-hydrostatic case (NPE)	12
2.3	Length scales	13
3	Proof of (hydrostatic) Theorem 1	14
3.1	The evolution of the enstrophy $\int_{\mathcal{V}} \zeta ^2 dV$	14
3.2	The evolution of $\int_{\mathcal{V}} \Theta_z ^2 dV$	19
3.3	Combination of the fluid and temperature inequalities	21
4	Proof of (non-hydrostatic) Theorem 2	23
5	Potential implications for simulations	24
A	Appendix A: Relations between ω, ζ and \mathfrak{w}	26
B	Appendix B: Inequalities	27
C	Appendix C: Proof of the L^3-Lemma	28

arXiv:0902.0066v2 [nlin.CD] 3 Mar 2009

Abstract

Recent advances in mathematical analysis by Cao and Titi (2005, 2007) and others have shown that solutions of the viscous hydrostatic primitive equations (HPE) on Neumann-like boundary conditions are, in fact, regular. In contrast, the regularity of non-hydrostatic primitive equations (NPE) solutions remains an open question. Our first aim in the present paper is to examine whether the establishment of its regularity still allows extreme events to arise spontaneously in HPE solutions. Such extreme events could include, for example, the sudden appearance and disappearance of locally intense fronts that do not involve deep convection. Our second aim is to determine what additional assumptions would be needed in the mathematical analysis to establish a similar result for NPE. Thus, we examine and contrast the two viscous PE models – hydrostatic (HPE) and non-hydrostatic (NPE) – in the light of the newly found mathematical regularity of HPE. Analytical methods are used to show that for both HPE and NPE the creation of small-scale structures is allowed locally in space and time at sizes that scale inversely with Reynolds number.

Summary: Richardson’s hydrostatic primitive equations (HPE) have formed the foundation of most numerical weather, climate and global ocean circulation predictions for many decades. The HPE govern incompressible, rotating, stratified fluid flows that are in hydrostatic balance. This balance is broken, however, in *deep convection* which occurs in cloud formation, flows over mountains and vertical fluid entrainment by strong gravity currents.

Independently of these operational issues, recent advances in mathematical analysis by Cao and Titi [29, 30], Kobelkov [31, 32] and Ju [34] have shown that solutions of the viscous HPE on Neumann-like boundary conditions are, in fact, regular. In contrast, the regularity of non-hydrostatic primitive equations (NPE) solutions remains an open question.

Thus, we examine and contrast the two viscous PE models – hydrostatic (HPE) and non-hydrostatic (NPE) – in the light of the newly found mathematical regularity of HPE. Analytical methods are used to show that for both HPE and NPE the creation of point-wise small-scale structures is allowed. More specifically, solutions behave differently in two distinct space-time regions \mathbb{S}^+ and \mathbb{S}^- . Very large lower bounds occur within the disjoint set \mathbb{S}^- on the double mixed derivatives of components of the velocity field (u_1, u_2, u_3) such as $|\partial^2 u_1 / \partial x_2 \partial x_3|$. Conversion of these results into point-wise inverse length-scales $\lambda_{(H,N)}^{-1}$ for either HPE or NPE on solutions within \mathbb{S}^- (if it is non-empty) shows that in both cases these scales have a lower bound that can be expressed as a linear sum of *local* horizontal and vertical Reynolds numbers, a local Rayleigh number and the global Reynolds number Re

$$L\lambda_{(H,N)}^{-1} \gtrsim c_{u_{hor}} \mathcal{R}_{u_{hor}} + c_{u_3} \mathcal{R}_{u_3} + c_{1,T} \mathcal{R}_{a,T} + c_{2,T} Re^{2/3} \mathcal{R}_{a,T}^{1/3} + \text{forcing},$$

where $c_{u_{hor}}$, c_{u_3} and $c_{i,T}$ are constants. The estimates of $L\lambda_{(H,N)}^{-1}$ for HPE and NPE, respectively, take the same form but have different coefficients. The vertical Reynolds number also contributes less in the hydrostatic case. The main differences in the analyses of HPE and NPE are that: (i) the known regularity of solutions for HPE must be assumed for NPE; and (ii) Neumann boundary conditions raise difficulties in the estimates for NPE that are not encountered for HPE. These difficulties are avoided here by imposing periodic boundary conditions on the NPE velocity field and its derivatives.

1 General Introduction

1.1 Introductory remarks

The hydrostatic primitive equations (HPE) were developed more than eighty years ago by Richardson [1] as a model for large-scale oceanographic and atmospheric dynamics. In this context, the *hydrostatic approximation* is the most reliable and accurate of all the assumptions made in applying them to operational numerical weather prediction (NWP), climate modelling and global numerical simulations of ocean circulation. The approximation arises from a scale analysis of synoptic systems; see [2, 3, 4, 5, 6, 7, 8, 9, 10, 11, 12, 13, 14, 15, 16, 17]. Basically, it neglects the vertical acceleration term in the vertical momentum equation. Physically, this enforces a perfect vertical force balance between gravity and the vertical pressure gradient force, which means that the pressure at a given location is given by the weight of the fluid above.

Until recently, the resolution of operational NWP models has been limited by computing power and operational time constraints to resolutions in which the hydrostatic approximation is almost perfectly valid. Operational forecasts therefore have relied mainly on hydrostatic models, which applied extremely well in numerical simulations of the global circulation of both the atmosphere and the ocean at the spatial and temporal resolutions that were available at the time. Meanwhile, the development of non-hydrostatic atmospheric models, which retain the vertical acceleration term and thus capture strong vertical convection, has been pursued over a period of more than four decades, especially for mesoscale investigations of sudden storms. As computer systems have become faster and memory has become more affordable over the past decade, there has been a corresponding increase in the spatial resolution of both NWP and climate simulation models. This improvement has facilitated a transition of the highly developed hydrostatic models towards non-hydrostatic models. Over the past decade, atmospheric research institutions have begun replacing their operational hydrostatic models with non-hydrostatic versions [14, 15, 17, 18].

The impending “model upgrade” may be tested by comparing the solution properties of the existing hydrostatic model at the new higher resolutions with those of its non-hydrostatic alternative. Using the fastest supercomputers available, global simulations of atmospheric circulation at resolutions of about 10 km in the horizontal (in the region of the hydrostatic limit) have recently been performed [19, 20]. These simulations were carried out only using hydrostatic models, as the non-hydrostatic versions were still under development. Perhaps not unexpectedly, the simulations at finer resolution found much more fine-scale structure than had been seen previously. More importantly, the smallest coherent features found at the previous coarser limits of resolution were *no longer present* at the finer resolution, because the balance between nonlinearity and dissipation that had created them previously was no longer being enforced. Instead, it was being enforced at the new limits of resolution.

Consequently, an important conclusion from these PE simulations was that the transition from the existing hydrostatic model to its non-hydrostatic alternative, and the distinction between their solutions, will require in both cases a much better understanding of the formation

of fine-scale frontal structures [20, 21]. For discussions of the history of ideas in fronto-genesis see [22, 26, 27, 28]. An example of wind measurements in a ‘gust front’ are found in Figure 1 [42, 16]. Gust fronts are indicated by ‘bow echoes’ on Döppler radar. These have been extensively observed and studied as the precursors of severe local weather [43, 44, 45, 46].

In particular, the physical parameterizations in the hydrostatic model are likely to require dramatic changes when simulated at the new finer resolutions. Therefore, in order to obtain the full benefit of the potential increase in accuracy provided by such high spatial resolution when using the non-hydrostatic model, one must first determine the range of solution behavior arising at the finer resolution in the computations of the previous hydrostatic model [20]. Over relatively small domains, operational model resolutions in the atmosphere are in fact already beyond the hydrostatic limit. These models run at resolutions finer than 10 km , where convection is partially resolved (thus, inaccurately simulated) by non-hydrostatic models. However, convection can only be fully resolved at model resolutions of about two orders of magnitude finer, that is, about 100 m or less in the horizontal. It is therefore likely that, for many years to come, operational hydrostatic and non-hydrostatic models will function at resolutions where convection can only be partially resolved. Consequently, the distinction between hydrostatic and non-hydrostatic solution behavior at these intermediate resolutions becomes paramount for the accuracy, predictability, reliability and physical interpretation of results in NWP. Against

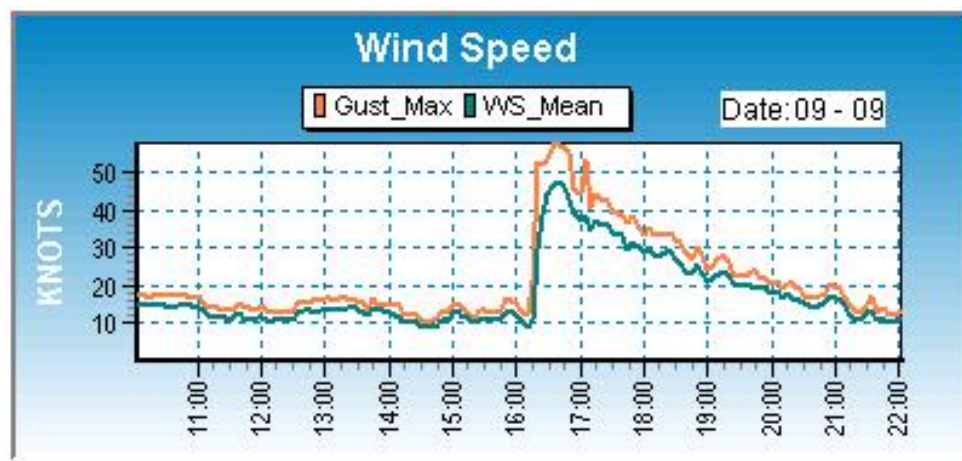


Figure 1: An example of a gust front manifesting itself in a sudden rise in wind speed [42, 16].

this background of renewed interest in the improvement of hydrostatic models and their newly acquired computability at higher resolution, this paper reports on the development of new analytical ideas that demonstrate the possibility of ‘extreme events’ (front formation, for example) occurring in solutions of both the hydrostatic (HPE) and non-hydrostatic (NPE) Primitive Equations. These events occur over very short space and time scales. While the problem of regularity of solutions – that is, the existence and uniqueness of strong solutions – in the viscous NPE remains open,¹ it has recently been shown by Cao and Titi [29, 30] and Kobelkov [31, 32], using

¹This is closely related to the open regularity problem for the three-dimensional Navier-Stokes equations which

independent methods, that solutions of the viscous HPE are regular.² Ju [34] then built on this result to show that these equations actually possess a global attractor, which means that the bounds are constants although no explicit estimates have been given. Considering the technical difficulties of this problem, which has been solved on a cylindrical domain with Neumann-type boundary conditions on the top and bottom, these results must be classed as a major advance.³ The significance of this result is that the status of solutions (existence and uniqueness) of the viscous HPE is now guaranteed: no singularities of any type can form in the solutions. However, a proof of the regularity solutions does *not* preclude the occurrence of “extreme events”. This term should not be interpreted in the present context in a statistical sense; rather, as the spontaneous appearance and disappearance of local, sudden, intermittent events with large gradients. These events would register as spatially localized, intense concentrations of vorticity, strain, and strong variations in temperature despite the fact that solutions ultimately remain smooth. The conventional approach to PDEs has been to prove bounded-ness of norms which, by their nature as volume integrals, tend to obscure the fine structure in a solution. The method used in this paper, first used to estimate intermittency in Navier-Stokes turbulence [35], is to search for fine structure in both versions of the PE by examining the *local* in behaviour of solutions in space-time. The ultimate aim is to explain fine-structure processes such as those that occur in fronto-genesis. The reader is referred to the work of Hoskins [26, 28] for general background on this phenomenon. While regularity is guaranteed for the viscous HPE, the problem remains open for the NPE and would need to be assumed. The assumption of regularity for NPE is not to be made lightly, but it is required in order to allow comparisons to be made between the two cases of HPE and NPE. This issue is discussed further in §2.

The mathematical approach is to show that solutions of both HPE and NPE may be divided into two space-time regions \mathbb{S}^+ and \mathbb{S}^- . If \mathbb{S}^- is non-empty then *very large lower bounds* on double mixed derivatives of components of the velocity field (u_1, u_2, u_3) such as $|\partial^2 u_1 / \partial x_3 \partial x_2|^2$ or $|\partial^2 u_2 / \partial x_1 \partial x_3|^2$ may occur within \mathbb{S}^- . These large point-wise lower bounds on second-derivative quantities represent intense accumulation in the (x_1, x_3) - and (x_2, x_3) -planes, respectively. Clearly, if solutions of great intensity were to accumulate in regions of the space-volume, this could only be allowed for finite times, in local spatial regions. Thus one would see the spontaneous formation of a front-like object localised in space that would only exist for a finite time. More specifically, the lower bounds within \mathbb{S}^- referred to above are a linear sum of $\mathcal{R}_{u_{hor}}^6$, $\mathcal{R}_{u_3}^6$ and $\mathcal{R}_{a,T}^6$ where $\mathcal{R}_{u_{hor}}$ and \mathcal{R}_{u_3} are *local* Reynolds numbers. That is, they are defined using the local space-time values of $u_{hor}(x_1, x_2, x_3, \tau) = \sqrt{u_1^2 + u_2^2}$ and the vertical velocity $u_3 = u_3(x_1, x_2, x_3, \tau)$. Likewise, $\mathcal{R}_{a,T}$ is a local Rayleigh number, defined using the local temperature $T(x_1, x_2, x_3, \tau)$. In contrast, Re is the global Reynolds number. For both HPE and NPE, these lower bounds within the \mathbb{S}^- -regions can be converted into lower bounds on the two

has been solved only for very thin domains ($0 < \alpha_a \ll 1$): see [36, 37, 38].

²Cao and Titi [29, 30] and Kobelkov [31, 32] proved that solutions are bounded for every finite time.

³Unfortunately the methods used for HPE do not extend to the three-dimensional Navier-Stokes equations; although HPE had been thought to be the more difficult of the two. See Lions, Temam and Wang [39, 40, 41].

point-wise inverse length scales $\lambda_{(H,N)}$

$$L\lambda_{(H,N)}^{-1} > c_{u_{hor}}\mathcal{R}_{u_{hor}} + c_{u_3}\mathcal{R}_{u_3} + c_{1,T}\mathcal{R}_{a,T} + c_{2,T}Re^{2/3}\mathcal{R}_{a,T}^{1/3} + \text{forcing} \quad (1.1)$$

although the constants $c_{u_{hor}}$, c_{u_3} and $c_{i,T}$ are different in each of the two cases. In the hydrostatic case \mathcal{R}_{u_3} may be negligible compared to $\mathcal{R}_{u_{hor}}$ but in the non-hydrostatic case its contribution may be significant in regions of strong vertical convection. The HPE-estimate for λ_H in (1.1) is of the order of a *metre* or less, at high Reynolds numbers. Our interpretation of this very small length is not that it is necessarily the thickness of a front, but that it may refer to the smallest scale of features *within* a front. The estimate of the allowed length-scale λ_N for NPE may be considerably less than λ_H for HPE, because \mathcal{R}_{u_3} in (1.1) is expected to make a more important contribution for NPE.

The methods employed in obtaining these estimates are identical in both cases but, while the regularity of solutions is assured for the HPE case, this property needs to be *assumed* for the NPE. Moreover, the restoration of the u_3 -term in the dynamics in NPE case causes difficulties in imposing the Neumann-type boundary conditions on the cylinder. These difficulties were avoided here by reverting to a periodic domain. The $T_z = 0$ temperature condition on the top and bottom was preserved. The key feature is the use of enstrophy (i.e. vorticity squared) rather than kinetic energy as a quadratic measure of motion. This means that the pressure gradient is excluded from the dynamics at an early stage, and - more importantly - that the analysis is immediately in terms of spatial derivatives of velocity components rather than the components themselves. In contrast, earlier approaches based available potential energy include the pressure field until a global spatial integral removes it and this has made local results more difficult to reach. In addition, energy arguments deliver results about attainable velocities not about velocity gradients.

<i>Quantity</i>	<i>Symbol</i>	<i>Definition</i>
Typical horizontal length	L	
Typical vertical length	H	
Typical temperature	T_0	
Aspect ratio	α_a	$\alpha_a = H/L$
Typical velocity	U_0	
twice vertical rotation rate	f	
Global Reynolds number	Re	$Re = U_0L\nu^{-1}$
Rossby number	ε	$\varepsilon = U_0(Lf)^{-1}$
Rayleigh number	R_a	$R_a = g\alpha T_0 H^3(\nu\kappa)^{-1}$
Hydrostatic const	a_0	$a_0 = \varepsilon\sigma\alpha_a^{-3}R_aRe^{-2}$
Frequency	ω_0	$\omega_0 = U_0L^{-1}$

Table 1: Definition of symbols for the primitive equations.

	<i>Dimensionless</i>	<i>Dimensional</i>	<i>Relation</i>
Horiz co-ords	x, y	x_1, x_2	$(x, y) = (x_1, x_2)L^{-1}$
Vertical co-ord	z	x_3	$z = x_3H^{-1}$
Time	t	τ	$t = \tau U_0 L^{-1}$
Horiz velocities	(u, v)	$\mathbf{u} = (u_1, u_2)$	$(u, v) = (u_1, u_2)U_0^{-1}$
Vertical velocity	w	u_3	$\alpha_a \varepsilon w = u_3 U_0^{-1}$
Velocity vector	$\mathbf{V} = (u, v, \varepsilon w)$		
Hydro-Velocity	$\mathbf{v} = (u, v, 0)$		
Non-Hydro-Vel	$\mathbf{v} = (u, v, \alpha_a^2 \varepsilon w)$		
Temperature	Θ	T	$\Theta = TT_0^{-1}$
2D-Gradient	$\nabla_2 = i\partial_x + j\partial_y$		
3D-Gradient	$\nabla_3 = i\partial_x + j\partial_y + k\partial_z$	$\nabla = i\partial_{x_1} + j\partial_{x_2} + k\alpha_a\partial_{x_3}$	$\nabla_3 = L\nabla$
3D-Laplacian	$\Delta_3 = \partial_x^2 + \partial_y^2 + \partial_z^2$		
Vorticity	$\boldsymbol{\omega} = \text{curl } \mathbf{V}$	$\boldsymbol{\Omega}$	$\boldsymbol{\Omega}_3 = \omega_3 \omega_0$
Hydro-vorticity	$\boldsymbol{\zeta} = \text{curl } \mathbf{v}$		
Non-hydro-vorticity	$\boldsymbol{\mathfrak{v}} = \text{curl } \mathbf{v}$		
Wind stress	\mathbf{s}	\mathbf{S}	
Heat transport	q	Q	

Table 2: Connection between dimensionless & dimensional variables.

In what follows, *dimensionless* co-ordinates are denoted by (x, y, z, t) . These are related to *dimensional* variables (x_1, x_2, x_3, τ) through the horizontal length scale L , the vertical length scale H : Table 1 gives the various standard definitions. Table 2 gives the notation concerning dimensionless and dimensional variables and some of the relations between them.

Dimensionless versions of both the HPE and NPE are expressed in terms of a set of velocity vectors based on the two horizontal velocities (u, v) and the vertical velocity w . These form the basis for the three-dimensional vector⁴

$$\mathbf{V}(x, y, z, t) = (u, v, \varepsilon w), \quad (1.2)$$

satisfying $\text{div } \mathbf{V} = 0$ or $u_x + v_y = -\varepsilon w_z$. The hydrostatic velocity vector is defined by

$$\mathbf{v} = (u, v, 0), \quad (1.3)$$

and the non-hydrostatic velocity vector by

$$\mathbf{v} = (u, v, \alpha_a^2 \varepsilon w), \quad (1.4)$$

where α_a is the aspect ratio defined in Table 3. Neither \mathbf{v} nor \mathbf{v} are divergence-free.

⁴ Comparing with the notation in [9], $(u, v) \equiv \mathbf{u}_2$ while $\mathbf{V} \equiv \mathbf{u}_3$ and $\mathbf{v} \equiv \mathbf{v}_3$.

The HPE that are studied in this paper should be compared with the modellers' HPE (MHPE) used by Richardson and incorporated in many numerical weather prediction and climate simulation models to this day. While the MHPE are written for a compressible fluid in the non-Euclidean geometry of a shallow atmosphere (i.e. the domain of flow is a spherical shell of constant radius, although vertical extent and motion are allowed) the HPE as laid out in Section 1.2 are written for an incompressible fluid in a Cartesian geometry. The 'incompressibility' of hydrostatic models appears when pressure is used as vertical coordinate. Hoskins and Bretherton [27] used a function of pressure to define a vertical coordinate that delivers the hydrostatic primitive equations for a compressible fluid that are nearly isomorphic to those for an incompressible fluid when ordinary height is used as vertical coordinate. They then introduced an approximation in the continuity equation that made the near isomorphism exact. The resulting HPE have frequently been used in theoretical studies and have led to many important results, but they are not identical to the MHPE that numerical modellers since Richardson have typically used.

1.2 Hydrostatic primitive equations (HPE)

The HPE in dimensionless form for the two horizontal velocities u and v are

$$\varepsilon \left(\frac{\partial}{\partial t} + \mathbf{V} \cdot \nabla_3 \right) u - v = \varepsilon Re^{-1} \Delta_3 u - p_x, \quad (1.5)$$

and

$$\varepsilon \left(\frac{\partial}{\partial t} + \mathbf{V} \cdot \nabla_3 \right) v + u = \varepsilon Re^{-1} \Delta_3 v - p_y. \quad (1.6)$$

There is no evolution equation for the vertical velocity w which lies in both $\mathbf{V} \cdot \nabla_3$ and the incompressibility condition $\text{div } \mathbf{V} = 0$. The z -derivative of the pressure field p and the dimensionless temperature Θ enter the problem through the hydrostatic equation

$$a_0 \Theta + p_z = 0. \quad (1.7)$$

The hydrostatic velocity field $\mathbf{v} = (u, v, 0)$ appears when (1.5), (1.6) and (1.7) are combined to form

$$\varepsilon \left(\frac{\partial}{\partial t} + \mathbf{V} \cdot \nabla_3 \right) \mathbf{v} + \mathbf{k} \times \mathbf{v} + a_0 \mathbf{k} \Theta = \varepsilon Re^{-1} \Delta_3 \mathbf{v} - \nabla_3 p, \quad (1.8)$$

together with the incompressibility condition $\text{div } \mathbf{v} = -\varepsilon w_z$. The dimensionless temperature⁵ Θ , with a specified heat transport term $q(x, y, z, t)$, satisfies

$$\left(\frac{\partial}{\partial t} + \mathbf{V} \cdot \nabla_3 \right) \Theta = (\sigma Re)^{-1} \Delta_3 \Theta + q. \quad (1.9)$$

The chosen domain is a cylinder, labelled $C(L, H)$, of height H ($0 \leq z \leq H$) and radius L . In terms of dimensionless variables, boundary conditions are taken to be:

⁵ Note that we use the upper-case Θ for the temperature to avoid confusion with lower-case θ which is conventionally used for the potential temperature.

1. On the cylinder bottom S^- at $z = 0$ the normal derivatives satisfy $u_z = v_z = \Theta_z = 0$ together with $w = 0$.
2. On its top S^+ at $z = H$, $(u_z, v_z) = \mathbf{s}(x, y)$, a specified wind-stress, with $\Theta_z = 0$ and $w = 0$. $\mathbf{s} \neq 0$ would be appropriate in the case of the ocean. For the atmosphere a choice of $\mathbf{s} = 0$ would be more appropriate, with the heat transport term $q(x, y, t)$ in (1.9) being the more dominant term.
3. Periodic boundary conditions on all variables are taken on the side of the cylinder S_C , which is a minor change from those in [29, 30, 34].

1.3 Non-hydrostatic primitive equations (NPE)

The NPE restore vertical acceleration so that, in contrast to (1.7), the equation for w reads

$$\alpha_a^2 \varepsilon^2 \left(\frac{\partial}{\partial t} + \mathbf{V} \cdot \nabla_3 \right) w + a_0 \Theta + p_z = \varepsilon R e^{-1} \Delta_3 w. \quad (1.10)$$

Using the definition of \mathbf{v} in (1.4) and putting (1.10) together with (1.5) and (1.6) we find

$$\varepsilon \left(\frac{\partial}{\partial t} + \mathbf{V} \cdot \nabla_3 \right) \mathbf{v} + \mathbf{k} \times \mathbf{v} + a_0 \mathbf{k} \Theta = \varepsilon R e^{-1} \Delta_3 \mathbf{v} - \nabla_3 p. \quad (1.11)$$

The equation for the temperature (1.9) remains the same. In contrast to the hydrostatic case where regularity has been established with realistic Neumann-type boundary conditions on the top of a cylinder, two questions remain open in the non-hydrostatic case :

1. No proof yet exists for the regularity of the NPE (1.11). Their prognostic equation for w brings NPE much closer to the three-dimensional Navier-Stokes equations for a rotating stratified fluid than the hydrostatic case, in which w is diagnosed from the incompressibility condition. While regularity properties for Navier-Stokes fluids on very thin domains ($0 < \alpha_a \ll 1$) have been established [36, 37], the general regularity problem remains open.
2. The boundary integrals for HPE estimated on the top and bottom of the cylinder $C(H, L)$ are problematic for NPE. Whereas the vorticity ζ in the hydrostatic case has only terms u_z and v_z in the horizontal components, which are specified on the top and bottom of $C(H, L)$, the non-hydrostatic vorticity

$$\mathbf{w} = \text{curl } \mathbf{v} \quad (1.12)$$

also includes w_x and w_y -terms which are not specified there. Surface integrals arising from the Laplacian also give trouble. Under these circumstances we have reverted to periodic boundary conditions on u , v and w and their derivatives on all parts of the cylinder. However, the temperature boundary conditions $\Theta_z = 0$ on the top/bottom of the cylinder with periodic on the side has been retained.

3. To address the influence of the material derivative in (1.10), typical values of $\alpha_a^2 \varepsilon^2$ can be determined. Typical observed values for mid-latitude synoptic weather and climate systems are:

$$\begin{aligned}\alpha_a &= H/L \approx 10^4 m / 10^6 m \approx 10^{-2} \\ W/U &\approx 10^{-2} m s^{-1} / 10 m s^{-1} \approx 10^{-3} \\ \varepsilon &= U/(f_0 L) \approx 10 m s^{-1} / (10^{-4} s^{-1} 10^6 m) \approx 10^{-1}.\end{aligned}\tag{1.13}$$

For mid-latitude large-scale ocean circulation, the corresponding numbers are:

$$\begin{aligned}\alpha_a &= H/L \approx 10^3 m / 10^5 m \approx 10^{-2} \\ W/U &\approx 10^{-3} m s^{-1} / 10^{-1} m s^{-1} \approx 10^{-2} \\ \varepsilon &= U/(f_0 L) \approx 10^{-1} m s^{-1} / (10^{-4} s^{-1} 10^5 m) \approx 10^{-2}.\end{aligned}\tag{1.14}$$

Thus, for these typical conditions, $\alpha_a^2 \varepsilon^2 \approx 10^{-8} - 10^{-6} \ll 1$ so the hydrostatic approximation can be expected to be extremely accurate in calculations of either synoptic weather and climate, or large-scale ocean circulation at mid-latitude.

2 The main results & their interpretation

The proof of global existence and uniqueness of solutions of HPE guarantees that at each point in space time a unique solution exists [30, 31, 32, 34]. In this section the results of two theorems, one for each case, are stated but the proofs are relegated to §3 and §4 respectively. The regularity problem remains open for NPE so this property is made as an assumption – see Theorem 2. It will be shown that solutions of great intensity are allowed to accumulate in regions of the space-volume \mathbb{S}^- which may only be allowed for finite times. Potentially these could represent the formation of fronts if appropriate temperature changes take place.

2.1 Results in the hydrostatic case (HPE)

Consider the arbitrary positive constants $0 < \delta_1, \delta_2 < 1$ chosen such that

$$\delta_3 = \frac{1}{2} \left(1 - \frac{3}{2} \delta_1 - \frac{1}{2} \delta_2 \right) > 0.\tag{2.1}$$

These are used to define a hydrostatic forcing function $F_H(Q, \mathbf{S})$:

$$\begin{aligned}F_H(Q, \mathbf{S}) &= \varepsilon^{-2} \left(\frac{1}{2} + \delta_2 + \frac{1}{2\delta_2} \right) Re^2 \mathcal{R}_{u_{hor}}^2 + \frac{\sigma}{6\delta_3 T_0^2 \omega_0^2} Re |Q|^2 \\ &+ \left(\frac{3}{2} \delta_1 + \frac{1}{2\delta_2} \right) \omega_0^{-2} Re^2 |\mathbf{S}|^2 + \frac{1}{2} \varepsilon^2 \omega_0^{-4} Re^2 |\mathbf{S}|^4 + \frac{L^{-1}}{2\omega_0^2} G_{S^+}(\Omega_3, \mathbf{S})\end{aligned}\tag{2.2}$$

where the surface integral is given by

$$G_{S^+}(\Omega_3, \mathbf{S}) = \int_{S^+} (\mathbf{k} \cdot \text{curl } \mathbf{S}) \Omega_3 dx_1 dx_2.\tag{2.3}$$

HPE quantity	Definition
Local (horiz) Reynolds no in terms of $ \mathbf{u} $	$\mathcal{R}_{u_{hor}} = L \mathbf{u} \nu^{-1}$
Local (vert) Reynolds no in terms of $ u_3 $	$\mathcal{R}_{u_3} = L u_3 \nu^{-1}$
Local Rayleigh no in terms of T	$\mathcal{R}_{a,T} = g\alpha H^3 T(\nu\kappa)^{-1}$
β_1	$\beta_1 = 2L^2\delta_3\omega_0^{-2}$
β_2	$\beta_2 = L^4(1 - 2\delta_3)\sigma^{-1}T_0^{-2}$
$\beta_{u_{hor}}$	$\beta_{u_{hor}} = \frac{20}{3\delta_1^3} + \frac{243}{32\delta_3^3}$
β_{u_3}	$\beta_{u_3} = \left(\frac{10}{3\delta_1^3} + \frac{\sigma^2}{12\delta_3^3}\right)$
$\beta_{1,T}$	$\beta_{1,T} = \frac{\sigma^2}{6} \left(1 + \frac{\sigma}{64}\right) \alpha_a^{-6} \delta_3^{-3}$
$\beta_{2,T}$	$\beta_{2,T} = \frac{\varepsilon^{-2} \alpha_a^{-6}}{2\delta_2}$
\mathcal{V}_*	$\mathcal{V}_* = \pi L^2 H \tau_*$

Table 3: Definitions in the hydrostatic case.

The main result is in Theorem 1 below where the spatially global quantity $\mathcal{H}(t)$

$$\mathcal{H}(t) = Re^3 \int_{\mathcal{V}} |\zeta|^2 dV + Re \int_{\mathcal{V}} |\Theta_z|^2 dV. \quad (2.4)$$

is used in the proof of the following theorem:

Theorem 1 (Hydrostatic case:) *In $C(H, L)$ over some chosen time interval $[0, \tau_*]$, the space-time 4-integral satisfies*

$$\begin{aligned} & \int_0^{\tau_*} \int_{\mathcal{V}} \left\{ -\beta_1 \left[|\nabla\Omega_3|^2 + \alpha_a^2 \left| \frac{\partial^2 u_1}{\partial x_2 \partial x_3} \right|^2 + \alpha_a^2 \left| \frac{\partial^2 u_2}{\partial x_1 \partial x_3} \right|^2 \right] - \beta_2 \alpha_a^2 |\nabla T_{x_3}|^2 \right. \\ & \quad + \beta_{u_1} \mathcal{R}_{u_{hor}}^6 + \beta_{u_3} \mathcal{R}_{u_3}^6 + \beta_{1,T} \mathcal{R}_{a,T}^6 + \beta_{2,T} Re^4 \mathcal{R}_{a,T}^2 \\ & \quad \left. + F_H(Q, \mathbf{S}) + \frac{1}{2} \mathcal{V}_*^{-1} \mathcal{H}(0) \right\} dx_1 dx_2 dx_3 d\tau > 0 \end{aligned} \quad (2.5)$$

where the coefficients are given in Table 3.

Remark 1: The proof in §3 shows that the right hand side of (2.5) is, in fact, $\frac{1}{2} \mathcal{H}(\tau_*)$. Because solutions of HPE are regular this is bounded above for all values of τ_* . However, it also has a lower bound of zero which is what is used. Although it is not necessarily a good lower bound, it is uniform in τ_* . Regularity of solutions is also a necessity in order to extract point-wise functions from within the 4-integral in (2.5).

Remark 2: From the positivity of the 4-integral in Theorem 1 we conclude:

1. There are regions of space-time $\mathcal{S}^+ \subset \mathbb{R}^4$ on which

$$\begin{aligned} & \beta_1 \left[|\nabla\Omega_3|^2 + \alpha_a^2 \left| \frac{\partial^2 u_1}{\partial x_2 \partial x_3} \right|^2 + \alpha_a^2 \left| \frac{\partial^2 u_2}{\partial x_1 \partial x_3} \right|^2 \right] + \beta_2 \alpha_a^2 |\nabla T_{x_3}|^2 \\ & \leq \beta_{u_{hor}} \mathcal{R}_{u_{hor}}^6 + \beta_{u_3} \mathcal{R}_{u_3}^6 + \beta_{1,T} \mathcal{R}_{a,T}^6 + \beta_{2,T} Re^4 \mathcal{R}_{a,T}^2 + F_H(Q, \mathbf{S}) + O(\tau_*^{-1}) \end{aligned} \quad (2.6)$$

2. Potentially there are also regions of space-time $\mathbb{S}^- \subset \mathbb{R}^4$ on which⁶

$$\begin{aligned} & \beta_1 \left[|\nabla\Omega_3|^2 + \alpha_a^2 \left| \frac{\partial^2 u_1}{\partial x_2 \partial x_3} \right|^2 + \alpha_a^2 \left| \frac{\partial^2 u_2}{\partial x_1 \partial x_3} \right|^2 \right] + \beta_2 \alpha_a^2 |\nabla T_{x_3}|^2 \\ & > \beta_{u_{hor}} \mathcal{R}_{u_{hor}}^6 + \beta_{u_3} \mathcal{R}_{u_3}^6 + \beta_{1,T} \mathcal{R}_{a,T}^6 + \beta_{2,T} Re^4 \mathcal{R}_{a,T}^2 + F_H(Q, \mathbf{S}) + O(\tau_*^{-1}) \end{aligned} \quad (2.7)$$

3. The 4-integral in (2.5) above yields no more information other than the possibility of a non-empty set \mathbb{S}^- existing. It says nothing about the spatial or temporal statistics of the subsets of \mathbb{S}^- (which will have a sensitive τ_* -dependence) nor does it give any indication of their topology.

2.2 Results in the non-hydrostatic case (NPE)

<i>NPE quantity</i>	<i>Definition</i> $0 < \eta_1 + \eta_2 < 1$
γ_1	$\gamma_1 = L^2(1 - \eta_1 - \eta_2)\omega_0^{-2}$
γ_2	$\gamma_2 = L^4(1 - \frac{1}{4}\eta_1)\sigma^{-1}T_0^{-2}$
$\gamma_{u_{hor}}$	$\gamma_{u_{hor}} = 4016\eta_1^{-3}$
γ_{u_3}	$\gamma_{u_3} = \eta_1^{-3} \left(\frac{\sigma^2}{12} + 1 \right)$
$\gamma_{1,T}$	$\gamma_{1,T} = \frac{32}{3} \left(\sigma^2 + \frac{\sigma^3}{16} \right) \eta_1^{-3}$
$\gamma_{2,T}$	$\gamma_{2,T} = \frac{\varepsilon^{-2}\alpha_a^{-6}}{2\delta_2}$
\mathcal{V}_*	$\mathcal{V}_* = \pi L^2 H \tau_*$

Table 4: Definitions in the non-hydrostatic case.

Now define the forcing function

$$F_{NH}(Q) = \frac{1}{2\varepsilon^2\eta_2} Re^2 \mathcal{R}_{u_{hor}}^2 + \frac{2\sigma}{T_0^2\omega_0^2\eta_1} Re|Q|^2 \quad (2.8)$$

The spatially global quantity $\mathcal{N}(t)$

$$\mathcal{N}(t) = Re^3 \int_{\mathcal{V}} |\mathbf{w}|^2 dV + Re \int_{\mathcal{V}} |\Theta_z|^2 dV \quad (2.9)$$

is used in the proof of the following theorem :

Theorem 2 (Non-hydrostatic case) *With periodic boundary conditions on the velocity variables and all their derivatives but with $T_z = 0$ on the top and bottom of the cylinder $C(H, L)$, assume that the non-hydrostatic equations have regular solutions. Then, over the chosen time interval $[0, \tau_*]$, the space-time 4-integral satisfies*

$$\begin{aligned} & \int_0^{\tau_*} \int_{\mathcal{V}} \left\{ -\gamma_1 |\nabla\Omega|^2 - \gamma_2 |\nabla T_{x_3}|^2 + \gamma_{u_1} \mathcal{R}_{u_{hor}}^6 + \gamma_{u_3} \mathcal{R}_{u_3}^6 \right. \\ & \quad \left. + \gamma_T \mathcal{R}_{a,T}^6 + \gamma_{2,T} Re^4 \mathcal{R}_{a,T}^2 + F_{NH}(Q) + \frac{1}{2} \mathcal{V}_*^{-1} \mathcal{N}(0) \right\} dx_1 dx_2 dx_3 d\tau > 0 \end{aligned} \quad (2.10)$$

⁶ Potentially large values of $|\nabla\Omega_3|$ in (2.7) also suggest the possibility of the formation of an Ekman-like layer : see Hide [23, 24, 25].

where the coefficients γ_i are given in Table 4.

Remark 1: Similar conclusions regarding the two regions of space-time \mathbb{S}^\pm can be drawn as in Theorem 1. Because of the presence of w in \mathbf{v} there are extra double derivatives in $|\nabla\Omega|^2$ not present in (2.5), so instead of attempting to write the negative terms in (2.10) as double mixed derivatives of the velocity field, $|\nabla\Omega|^2$ is left as it stands. §4 is devoted to the proof.

Remark 2: The proof in §4 shows that the right hand side of (2.10) is $\frac{1}{2}\mathcal{N}(\tau_*)$. It is here where regularity of solutions needs to be assumed because $\mathcal{N}(\tau_*)$ is required to be finite for every value of τ_* and we also wish to extract point-wise functions from within the 4-integral. It also has a lower bound of zero uniform in τ_* which is what is used in (2.10).

2.3 Length scales

To illustrate the nature of a front, very large values of double mixed-derivatives are required in local parts of the flow as envisaged in the early and pioneering work of Hoskins [26, 28]. For instance, very large values of $|\partial^2 u_1 / \partial x_3 \partial x_2|^2$ or $|\partial^2 u_2 / \partial x_3 \partial x_1|^2$ would represent intense accumulation in the (x_1, x_3) - and (x_2, x_3) -planes respectively. The boundaries of the front regions illustrated in Figure 1 below may pictorially represent a subset of \mathbb{S}^- .

The large lower bounds in both Theorems 1 and 2 can be interpreted in terms of a length scale. To achieve this, define the two point-wise inverse length scales $\lambda_{H,N}^{-1}$ such that⁷

$$(L\lambda_H^{-1})^6 = L^2\omega_0^{-2} \left(|\nabla\Omega_3|^2 + \alpha_a^2 \left| \frac{\partial^2 u_1}{\partial x_2 \partial x_3} \right|^2 + \alpha_a^2 \left| \frac{\partial^2 u_2}{\partial x_1 \partial x_3} \right|^2 \right) + \alpha_a^2 \beta_2 \beta_1^{-1} L^4 |\nabla T_{x_3}|^2 T_0^{-2}, \quad (2.11)$$

and

$$(L\lambda_N^{-1})^6 = L^2 |\nabla\Omega|^2 \omega_0^{-2} + \gamma_2 \gamma_1^{-1} L^4 |\nabla T_{x_3}|^2 T_0^{-2}. \quad (2.12)$$

In each case one could define a more limited right hand side to reflect which term is dominant: however, (2.11) and (2.12) are left in their most general forms. The sixth-powers on the right hand sides of both Theorems 1 and 2 give results within \mathbb{S}^-

$$L\lambda_{(H,N)}^{-1} > c_{u_{hor}} \mathcal{R}_{u_{hor}} + c_{u_3} \mathcal{R}_{u_3} + c_{1,T} \mathcal{R}_{a,T} + c_{2,T} Re^{2/3} \mathcal{R}_{a,T}^{1/3} + \text{forcing} \quad \text{in} \quad \mathbb{S}^- \quad (2.13)$$

where the coefficients $c_{u_{hor}}$, c_{u_3} and $c_{i,T}$ can be calculated from Theorems 1 and 2 and will be different in both cases. (2.13) can be interpreted as a lower bound on the inverse length scale of the smallest feature in a front. As already noted, no information is available on any statistics nor on the shape and size of subsets of \mathbb{S}^- .

⁷The point-wise local length scales $\lambda_{H,N}^{-1}$ are formed in the same dimensional manner as the Kraichnan length ℓ_k , namely, from a combination of the palenstrophy $|\nabla\omega|^2$ and the viscosity ν given by $\ell_k^{-6} = \nu^{-2} |\nabla\omega|^2$.

3 Proof of (hydrostatic) Theorem 1

3.1 The evolution of the enstrophy $\int_{\mathcal{V}} |\zeta|^2 dV$

The vorticity $\zeta = \text{curl } \mathbf{v}$ is specifically given by

$$\zeta = \text{curl } \mathbf{v} = -i v_z + j u_z + \mathbf{k}(v_x - u_y). \quad (3.1)$$

This contains the same \mathbf{k} -component as the full 3D-vorticity $\zeta = \nabla_3 \times \mathbf{V}$ but with the w -terms missing. In the following certain standard vector identities are useful⁸. Appendix B shows that

$$-\mathbf{V} \cdot \nabla_3 \mathbf{v} = \mathbf{V} \times \zeta - \frac{1}{2} \nabla_3 (u^2 + v^2) \quad (3.5)$$

so taking the curl of (1.8) gives

$$\varepsilon \frac{\partial \zeta}{\partial t} = \varepsilon Re^{-1} \Delta_3 \zeta + \varepsilon \text{curl} (\mathbf{V} \times \zeta) - \text{curl} (\mathbf{k} \times \mathbf{v} + a_0 \mathbf{k} T). \quad (3.6)$$

This process has removed both gradient terms in (1.8) and (3.5) and allows us to write

$$\begin{aligned} \frac{1}{2} \varepsilon \frac{d}{dt} \int_{\mathcal{V}} |\zeta|^2 dV &= \varepsilon Re^{-1} \int_{\mathcal{V}} \zeta \cdot \Delta_3 \zeta dV + \varepsilon \int_{\mathcal{V}} \zeta \cdot \text{curl} (\mathbf{V} \times \zeta) dV \\ &\quad - \int_{\mathcal{V}} \zeta \cdot \text{curl} (\mathbf{k} \times \mathbf{v} + a_0 \mathbf{k} T) dV, \end{aligned} \quad (3.7)$$

without involving pressure terms. Firstly we begin with the second integral on the right hand side of (3.7)

$$\int_{\mathcal{V}} \zeta \cdot \text{curl} (\mathbf{V} \times \zeta) dV = \int_{\mathcal{V}} \text{curl } \zeta \cdot (\mathbf{V} \times \zeta) dV \mp \int_{S^\pm} \mathbf{k} \cdot \{\zeta \times (\mathbf{V} \times \zeta)\} dx dy.$$

However, on S^+ , $\mathbf{k} \times \zeta = -\mathbf{s}$ so we have

$$\left| \int_{\mathcal{V}} \zeta \cdot \text{curl} (\mathbf{V} \times \zeta) dV \right| \leq (\|\text{curl } \zeta\|_2 + \|\mathbf{s}\|_2) \|\mathbf{V}\|_6 \|\zeta\|_3 \quad (3.8)$$

Secondly, because $\text{div } \zeta = 0$

$$\begin{aligned} \int_{\mathcal{V}} \zeta \cdot \Delta_3 \zeta dV &= - \int_{\mathcal{V}} \zeta \cdot \text{curl curl } \zeta dV \\ &= - \int_{\mathcal{V}} |\text{curl } \zeta|^2 dV + \int_S \hat{\mathbf{n}} \cdot (\zeta \times \text{curl } \zeta) dS \end{aligned} \quad (3.9)$$

⁸Three useful vector identities are

$$\text{div} (\mathbf{A} \times \mathbf{B}) = \mathbf{B} \cdot \text{curl } \mathbf{A} - \mathbf{A} \cdot \text{curl } \mathbf{B}, \quad (3.2)$$

$$\nabla (\mathbf{A} \cdot \mathbf{B}) = \mathbf{A} \cdot \nabla \mathbf{B} + \mathbf{B} \cdot \nabla \mathbf{A} + \mathbf{A} \times \text{curl } \mathbf{B} + \mathbf{B} \times \text{curl } \mathbf{A}, \quad (3.3)$$

$$\text{curl} (\mathbf{A} \times \mathbf{B}) = \mathbf{A} \text{div } \mathbf{B} - \mathbf{B} \text{div } \mathbf{A} + \mathbf{B} \cdot \nabla \mathbf{A} - \mathbf{A} \cdot \nabla \mathbf{B}. \quad (3.4)$$

where S is the cylinder surface. This is zero on the sides S_C because of periodicity and on the top and bottom surfaces S_{\pm} it takes the values

$$\int_{S_{\pm}} \hat{\mathbf{n}} \cdot (\boldsymbol{\zeta} \times \text{curl } \boldsymbol{\zeta}) \, dx dy = \pm \int_{S_{\pm}} (\mathbf{k} \times \boldsymbol{\zeta}) \cdot \text{curl } \boldsymbol{\zeta} \, dx dy. \quad (3.10)$$

However, $\mathbf{k} \times \boldsymbol{\zeta} = -(\mathbf{i}u_z + \mathbf{j}v_z) = -\mathbf{s}$ on the upper and lower cylinder surfaces S_{\pm} . Therefore

$$\left| \int_{S_{\pm}} \hat{\mathbf{n}} \cdot (\boldsymbol{\zeta} \times \text{curl } \boldsymbol{\zeta}) \, dx dy \right| \leq \|\mathbf{s}\|_2 \|\text{curl } \boldsymbol{\zeta}\|_2, \quad (3.11)$$

Thirdly, from the vector identity (3.2) and the Divergence Theorem

$$\begin{aligned} \int_{\mathcal{V}} \boldsymbol{\zeta} \cdot \text{curl}(\mathbf{k} \times \mathbf{v} + a_0 \mathbf{k}T) \, dV &= \int_{\mathcal{V}} \text{curl } \boldsymbol{\zeta} \cdot (\mathbf{k} \times \mathbf{v} + a_0 \mathbf{k}T) \, dV \\ &\quad - \int_S \hat{\mathbf{n}} \cdot \{\boldsymbol{\zeta} \times (\mathbf{k} \times \mathbf{v} + a_0 \mathbf{k}T)\} \, dS \end{aligned} \quad (3.12)$$

The contribution from the sides of $C(H, L)$ to the full surface integral is zero because of periodicity, while the contribution from the top and bottom surfaces $\hat{\mathbf{n}} = \pm \mathbf{k}$ is zero for the last term. Because $\mathbf{k} \times \boldsymbol{\zeta} = -(\mathbf{i}u_z + \mathbf{j}v_z) = -\mathbf{s}$ on the upper and lower cylinder surfaces S_{\pm} we have

$$\left| - \int_{\mathcal{V}} \hat{\mathbf{n}} \cdot \{\boldsymbol{\zeta} \times (\mathbf{k} \times \mathbf{v})\} \, dV \right| \leq \left| \pm \int_{S_{\pm}} \mathbf{s} \cdot (\mathbf{k} \times \mathbf{v}) \, dx dy \right| \leq \|\mathbf{s}\|_2 \|\mathbf{v}\|_2. \quad (3.13)$$

Thus (3.7) is re-written as

$$\begin{aligned} \frac{1}{2} \varepsilon \frac{d}{dt} \int_{\mathcal{V}} |\boldsymbol{\zeta}|^2 \, dV &\leq -\varepsilon Re^{-1} \int_{\mathcal{V}} |\text{curl } \boldsymbol{\zeta}|^2 \, dV + \varepsilon (\|\text{curl } \boldsymbol{\zeta}\|_2 + \|\mathbf{s}\|_2) \|\mathbf{V}\|_6 \|\boldsymbol{\zeta}\|_3 \\ &\quad - \int_{\mathcal{V}} (\text{curl } \boldsymbol{\zeta}) \cdot (\mathbf{k} \times \mathbf{v} + a_0 \mathbf{k}\Theta) \, dV + \varepsilon Re^{-1} \|\mathbf{s}\|_2 \|\text{curl } \boldsymbol{\zeta}\|_2 + \|\mathbf{s}\|_2 \|\mathbf{v}\|_2 \\ &\equiv -\varepsilon Re^{-1} \int_{\mathcal{V}} |\text{curl } \boldsymbol{\zeta}|^2 \, dV + \text{T1} + \text{T2} + \text{T3} + \text{T4}, \end{aligned} \quad (3.14)$$

where

$$\text{T1} = \varepsilon (\|\text{curl } \boldsymbol{\zeta}\|_2 + \|\mathbf{s}\|_2) \|\mathbf{V}\|_6 \|\boldsymbol{\zeta}\|_3 \quad (3.15)$$

$$\text{T2} = - \int_{\mathcal{V}} (\text{curl } \boldsymbol{\zeta}) \cdot (\mathbf{k} \times \mathbf{v}) \, dV, \quad \text{T3} = -a_0 \int_{\mathcal{V}} (\text{curl } \boldsymbol{\zeta}) \cdot (\mathbf{k}\Theta) \, dV. \quad (3.16)$$

and

$$\text{T4} = \varepsilon Re^{-1} \|\mathbf{s}\|_2 \|\text{curl } \boldsymbol{\zeta}\|_2 + \|\mathbf{s}\|_2 \|\mathbf{v}\|_2 \quad (3.17)$$

Before estimating T1, T2, and T3, we prove

Lemma 1 *In the cylinder $C(H, L)$*

$$\|\boldsymbol{\zeta}\|_3 \leq \left(3^{1/2} \|\text{curl } \boldsymbol{\zeta}\|_2^{1/2} + \|\mathbf{s}\|_2^{1/2} \right) \|\mathbf{v}\|_6^{1/2}. \quad (3.18)$$

Proof: Consider

$$\begin{aligned}
\int_{\mathcal{V}} |\zeta|^3 dV &= \int_{\mathcal{V}} \zeta \cdot (\zeta \zeta) dV \\
&= \int_{\mathcal{V}} \mathbf{v} \cdot \operatorname{curl}(\zeta \zeta) dV - \int_S \operatorname{div}(\zeta(\mathbf{v} \times \zeta)) dS \\
&= \int_{\mathcal{V}} \mathbf{v} \cdot (\zeta \operatorname{curl} \zeta + (\nabla_3 \zeta) \times \zeta) dV \mp \int_{S^\pm} \mathbf{k} \cdot (\mathbf{v} \times \zeta) \zeta dS.
\end{aligned} \tag{3.19}$$

A vector identity

$$\nabla_3 \zeta = \frac{1}{2}(\zeta)^{-1} \nabla_3(\zeta \cdot \zeta) = \hat{\zeta} \cdot \nabla_3 \zeta + \hat{\zeta} \times \operatorname{curl} \zeta \tag{3.20}$$

gives

$$\begin{aligned}
\operatorname{curl}(\zeta \zeta) &= 2\zeta \operatorname{curl} \zeta - \hat{\zeta}(\zeta \cdot \operatorname{curl} \zeta) - \zeta \times (\hat{\zeta} \cdot \nabla_3 \zeta) \\
&= \zeta \operatorname{curl} \zeta + (\zeta \times \operatorname{curl} \zeta) \times \hat{\zeta} - \zeta \times (\hat{\zeta} \cdot \nabla_3 \zeta).
\end{aligned} \tag{3.21}$$

We also use the fact that $\mathbf{k} \times \zeta = -\mathbf{s}$ on S^+ to conclude

$$\begin{aligned}
\int_{\mathcal{V}} |\zeta|^3 dV &= \int_{\mathcal{V}} \mathbf{v} \cdot \left(\zeta \operatorname{curl} \zeta + (\zeta \times \operatorname{curl} \zeta) \times \hat{\zeta} - \zeta \times (\hat{\zeta} \cdot \nabla_3 \zeta) \right) dV \\
&\mp \int_{S^\pm} \mathbf{k} \cdot (\mathbf{v} \times \zeta) \zeta dS.
\end{aligned} \tag{3.22}$$

Using inequality (B.6) in Appendix B, we find

$$\int_{\mathcal{V}} |\zeta|^3 dV \leq 3 \|\operatorname{curl} \zeta\|_2 \|\zeta\|_3 \|\mathbf{v}\|_6 + \|\mathbf{s}\|_2 \|\zeta\|_3 \|\mathbf{v}\|_6 \tag{3.23}$$

giving the result (3.18). \square

Lemma 2 *Within the cylinder $C(L, H)$, $T1$, $T2$ and $T3$ are estimated as*

$$|T1| \leq \frac{3}{2} \delta_1 \varepsilon Re^{-1} \|\operatorname{curl} \zeta\|_2^2 + \frac{3}{2} \delta_1 \varepsilon Re^{-1} \|\mathbf{s}\|_2^2 + \frac{10\varepsilon}{3\delta_1^3} Re^3 (\|\mathbf{V}\|_6^6 + \|\mathbf{v}\|_6^6) \tag{3.24}$$

for any $\delta_1 > 0$. Moreover, for any $\delta_2 > 0$

$$|T2| \leq \frac{1}{2} \delta_2 \varepsilon Re^{-1} \|\operatorname{curl} \zeta\|_2^2 + \frac{1}{2} \delta_2^{-1} \varepsilon^{-1} Re \|\mathbf{v}\|_2^2, \tag{3.25}$$

$$|T3| \leq \frac{1}{2} \delta_2 \varepsilon Re^{-1} \|\operatorname{curl} \zeta\|_2^2 + \frac{a_0^2}{2\varepsilon \delta_2} Re \|\Theta\|_2^2, \tag{3.26}$$

and $\delta_2 > 0$

$$T4 \leq \varepsilon \delta_2 Re^{-1} \|\operatorname{curl} \zeta\|_2^2 + \delta_2 \varepsilon^{-1} Re \|\mathbf{v}\|_2^2 + \frac{\varepsilon}{2\delta_2} Re^{-1} \|\mathbf{s}\|_2^2. \tag{3.27}$$

Proof: In the following the $\delta_i > 0$ are constants introduced by a series of Young's inequalities – see (B.7) in Appendix B:

1) Using Lemma 1 T1 can be written as

$$\begin{aligned}
\text{T1} &= \varepsilon (\|\text{curl } \boldsymbol{\zeta}\|_2 + \|\mathbf{s}\|_2) \|\mathbf{V}\|_6 \|\boldsymbol{\zeta}\|_3 & (3.28) \\
&\leq \varepsilon (\|\text{curl } \boldsymbol{\zeta}\|_2 + \|\mathbf{s}\|_2) \|\mathbf{V}\|_6 \times \left(2^{1/2} \|\text{curl } \boldsymbol{\zeta}\|_2^{1/2} + \|\mathbf{s}\|_2^{1/2}\right) \|\mathbf{v}\|_6^{1/2} \\
&\leq (\delta_1 \varepsilon Re^{-1} \|\text{curl } \boldsymbol{\zeta}\|_2^2)^{3/4} (9\varepsilon \delta_1^{-3} Re^3 \|\mathbf{V}\|_6^6)^{1/6} (9\varepsilon \delta_1^{-3} Re^3 \|\mathbf{v}\|_6^6)^{1/12} \\
&\quad + (\delta_1 \varepsilon Re^{-1} \|\text{curl } \boldsymbol{\zeta}\|_2^2)^{1/2} (\delta_1 \varepsilon Re^{-1} \|\mathbf{s}\|_2^2)^{1/4} (\varepsilon \delta_1^{-3} Re^3 \|\mathbf{V}\|_6^6)^{1/6} (\varepsilon \delta_1^{-3} Re^3 \|\mathbf{v}\|_6^6)^{1/12} \\
&\quad + (\delta_1 \varepsilon Re^{-1} \|\text{curl } \boldsymbol{\zeta}\|_2^2)^{1/4} (\delta_1 \varepsilon Re^{-1} \|\mathbf{s}\|_2^2)^{1/2} (9\varepsilon \delta_1^{-3} Re^3 \|\mathbf{V}\|_6^6)^{1/6} (9\varepsilon \delta_1^{-3} Re^3 \|\mathbf{v}\|_6^6)^{1/12} \\
&\quad + (\delta_1 \varepsilon Re^{-1} \|\mathbf{s}\|_2^2)^{3/4} (\varepsilon \delta_1^{-3} Re^3 \|\mathbf{V}\|_6^6)^{1/6} (\varepsilon \delta_1^{-3} Re^3 \|\mathbf{v}\|_6^6)^{1/12} \\
&\leq \frac{3}{2} \delta_1 \varepsilon Re^{-1} \|\text{curl } \boldsymbol{\zeta}\|_2^2 + \frac{3}{2} \delta_1 \varepsilon Re^{-1} \|\mathbf{s}\|_2^2 + \frac{10\varepsilon}{3\delta_1^3} Re^3 (\|\mathbf{V}\|_6^6 + \|\mathbf{v}\|_6^6). & (3.29)
\end{aligned}$$

2) From (3.16), T2 can be estimated as

$$\begin{aligned}
|\text{T2}| &\leq \|\text{curl } \boldsymbol{\zeta}\|_2 \|\mathbf{v}\|_2 \\
&= (\delta_2 \varepsilon Re^{-1} \|\text{curl } \boldsymbol{\zeta}\|_2^2)^{1/2} (\delta_2^{-1} \varepsilon^{-1} Re \|\mathbf{v}\|_2^2)^{1/2} \\
&\leq \frac{1}{2} \delta_2 \varepsilon Re^{-1} \|\text{curl } \boldsymbol{\zeta}\|_2^2 + \frac{1}{2} \delta_2^{-1} \varepsilon^{-1} Re \|\mathbf{v}\|_2^2. & (3.30)
\end{aligned}$$

3) From (3.16), and using the same constant δ_2 , T3 is estimated as

$$\begin{aligned}
|\text{T3}| &\leq a_0 \|\text{curl } \boldsymbol{\zeta}\|_2 \|\Theta\|_2 = (\delta_2 \varepsilon Re^{-1} \|\text{curl } \boldsymbol{\zeta}\|_2^2)^{1/2} \left(\frac{a_0^2}{\delta_2 \varepsilon} Re \|\Theta\|_2^2\right)^{1/2} \\
&\leq \frac{1}{2} \delta_2 \varepsilon Re^{-1} \|\text{curl } \boldsymbol{\zeta}\|_2^2 + \frac{a_0^2}{2\delta_2 \varepsilon} Re \|\Theta\|_2^2. & (3.31)
\end{aligned}$$

4) The final group of terms in the Lemma can be broken up thus:

$$\begin{aligned}
\text{T4} = \varepsilon Re^{-1} \|\text{curl } \boldsymbol{\zeta}\|_2 \|\mathbf{s}\|_2 + \|\mathbf{s}\|_2 \|\mathbf{v}\|_2 &\leq \varepsilon \delta_2 Re^{-1} \|\text{curl } \boldsymbol{\zeta}\|_2^2 + \frac{\varepsilon}{4\delta_2} Re^{-1} \|\mathbf{s}\|_2^2 \\
&\quad + \frac{\varepsilon}{4\delta_2} Re^{-1} \|\mathbf{s}\|_2^2 + \delta_2 \varepsilon^{-1} Re \|\mathbf{v}\|_2^2 \\
&\leq \frac{1}{2} \varepsilon \delta_2 Re^{-1} \|\text{curl } \boldsymbol{\zeta}\|_2^2 + \delta_2 \varepsilon^{-1} Re \|\mathbf{v}\|_2^2 \\
&\quad + \frac{\varepsilon}{2\delta_2} Re^{-1} \|\mathbf{s}\|_2^2. & (3.32)
\end{aligned}$$

as advertised. \square

Dividing by ε and gathering terms gives

$$\begin{aligned}
\frac{1}{2} \frac{d}{dt} \int_{\mathcal{V}} |\boldsymbol{\zeta}|^2 dV &\leq -(1 - \frac{3}{2} \delta_1 - 2\delta_2) Re^{-1} \int_{\mathcal{V}} |\text{curl } \boldsymbol{\zeta}|^2 dV & (3.33) \\
&\quad + \frac{10}{3\delta_1^3} Re^3 (\varepsilon^6 \|w\|_6^6 + 2\|\mathbf{v}\|_6^6) + \frac{1}{\varepsilon^2} \left(\delta_2 + \frac{1}{2\delta_2}\right) Re \|\mathbf{v}\|_2^2 \\
&\quad + \frac{a_0^2}{2\varepsilon^2 \delta_2} Re \|\Theta\|_2^2 + \left(\frac{3}{2} \delta_1 + \frac{1}{2\delta_2}\right) Re^{-1} \|\mathbf{s}\|_2^2.
\end{aligned}$$

The following Lemma relates $\int_{\mathcal{V}} |\text{curl } \boldsymbol{\zeta}|^2 dV$ to sums of squares.

Lemma 3 Let ω_3 be the third component of the full vorticity $\boldsymbol{\omega} = \nabla_3 \times \mathbf{V} = (\omega_1, \omega_2, \omega_3)$ and let $G_{S^+}(\omega_3, \mathbf{s})$ on the top surface of the cylinder be defined as in (2.3) repeated below

$$G_{S^+}(\omega_3, \mathbf{s}) = \int_{S^+} (\mathbf{k} \cdot \text{curl } \mathbf{s}) \omega_3 \, dx dy. \quad (3.34)$$

Then for any $0 < \delta_0 < 1$, $\int_{\mathcal{V}} |\text{curl } \boldsymbol{\zeta}|^2 dV$ satisfies

$$\begin{aligned} \int_{\mathcal{V}} |\text{curl } \boldsymbol{\zeta}|^2 dV &> \min\{1, 2(1 - \delta_0)\} \int_{\mathcal{V}} |\nabla_3 \omega_3|^2 dV + 2\delta_0 \int_{\mathcal{V}} \{|u_{yz}|^2 + |v_{xz}|^2\} dV \\ &+ \int_{\mathcal{V}} \{|u_{zz}|^2 + |v_{zz}|^2 + \varepsilon^2(1 - \delta_0)|w_{zz}|^2\} dV - G_{S^+}(\omega_3, \mathbf{s}). \end{aligned} \quad (3.35)$$

Proof: Using $\boldsymbol{\zeta}$ in (3.1) in the form $\boldsymbol{\zeta} = -v_z \mathbf{i} + u_z \mathbf{j} + \omega_3 \mathbf{k}$ with $\omega_3 = v_x - u_y$ and recalling that $\varepsilon w_z = -(u_x + v_y)$

$$\text{curl } \boldsymbol{\zeta} = \begin{vmatrix} \mathbf{i} & \mathbf{j} & \mathbf{k} \\ \partial_x & \partial_y & \partial_z \\ -v_z & u_z & \omega_3 \end{vmatrix} = \mathbf{i}(\omega_{3,y} - u_{zz}) - \mathbf{j}(\omega_{3,x} + v_{zz}) - \varepsilon \mathbf{k} w_{zz} \quad (3.36)$$

Thus

$$|\text{curl } \boldsymbol{\zeta}|^2 = |\nabla_2 \omega_3|^2 + (u_{zz}^2 + v_{zz}^2 + \varepsilon^2 w_{zz}^2) - 2(\omega_{3,y} u_{zz} - \omega_{3,x} v_{zz}). \quad (3.37)$$

Now

$$-2 \int_{\mathcal{V}} (\omega_{3,y} u_{zz} - \omega_{3,x} v_{zz}) dV = 2 \int_{\mathcal{V}} |\omega_{3,z}|^2 dV + 2 \int_{S^+} \mathbf{s} \cdot (\mathbf{k} \times \nabla_3 \omega_3) dS \quad (3.38)$$

and

$$\begin{aligned} \int_{S^+} \mathbf{s} \cdot (\mathbf{k} \times \nabla_3 \omega_3) dx dy &= - \int_{S^+} \mathbf{s} \cdot \text{curl}(\mathbf{k} \omega_3) dx dy \\ &= - \int_{S^+} (\text{curl } \mathbf{s}) \cdot (\mathbf{k} \omega_3) dx dy + \int_{S^+} \text{div}(\omega_3 \mathbf{s} \times \mathbf{k}) dx dy. \end{aligned} \quad (3.39)$$

The last term can easily be turned into a closed line integral over the circular cylinder boundary on which we have periodicity. Thus it is zero and we have

$$-2 \int_{\mathcal{V}} (\omega_{3,y} u_{zz} - \omega_{3,x} v_{zz}) dV = 2 \int_{\mathcal{V}} |\omega_{3,z}|^2 dV - G_{S^+}(\omega_3, \mathbf{s}) \quad (3.40)$$

and so

$$\begin{aligned} \int_{\mathcal{V}} |\text{curl } \boldsymbol{\zeta}|^2 dV &= \int_{\mathcal{V}} \{|\nabla_3 \omega_3|^2 + |\omega_{3,z}|^2\} dV \\ &+ \int_{\mathcal{V}} \{u_{zz}^2 + v_{zz}^2 + \varepsilon^2 w_{zz}^2\} dV - G_{S^+}(\omega_3, \mathbf{s}) \end{aligned} \quad (3.41)$$

Moreover, it is easily shown that

$$\begin{aligned} \int_{\mathcal{V}} (\varepsilon^2 |w_{zz}|^2 + 2|\omega_{3,z}|^2) dV &= \int_{\mathcal{V}} \{(u_{xz} - v_{yz})^2 + 2(u_{yz}^2 + v_{xz}^2)\} dV \\ &> 2 \int_{\mathcal{V}} (u_{yz}^2 + v_{xz}^2) dV \end{aligned} \quad (3.42)$$

where a pair of horizontal integrations by parts in the first line of (3.42) have been performed. These have no boundary terms. A linear combination of (3.41) and (3.42) gives

$$\begin{aligned}
\int_{\mathcal{V}} |\operatorname{curl} \zeta|^2 dV &= \int_{\mathcal{V}} \{ |\nabla_2 \omega_3|^2 + 2|\omega_{3,z}|^2 dV \} - G_{S^+}(\omega_3, \mathbf{s}) \\
&+ \int_{\mathcal{V}} \{ u_{zz}^2 + v_{zz}^2 + \varepsilon^2 w_{zz}^2 \} dV \\
&> \int_{\mathcal{V}} \{ |\nabla_3 \omega_2|^2 + 2(1 - \delta_0)|\omega_{3,z}|^2 dV \} - G_{S^+}(\omega_3, \mathbf{s}) \\
&+ \int_{\mathcal{V}} \{ u_{zz}^2 + v_{zz}^2 + (1 - \delta_0)\varepsilon^2 w_{zz}^2 \} dV + 2\delta_0 \int_{\mathcal{V}} (u_{yz}^2 + v_{xz}^2) dV, \quad (3.43)
\end{aligned}$$

which gives (3.35). This completes the proof. \square

3.2 The evolution of $\int_{\mathcal{V}} |\Theta_z|^2 dV$

The partial differential equation for Θ given in (1.9) with BCs applied on $C(L, H)$

$$\frac{\partial \Theta}{\partial t} + \mathbf{V} \cdot \nabla_3 \Theta = (\sigma Re)^{-1} \Delta_3 \Theta + q \quad (3.44)$$

is now differentiated with respect to z to give

$$\begin{aligned}
\frac{1}{2} \frac{d}{dt} \int_{\mathcal{V}} |\Theta_z|^2 dV &= (\sigma Re)^{-1} \int_{\mathcal{V}} \Theta_z (\Delta_3 \Theta_z) dV - \int_{\mathcal{V}} \Theta_z \frac{\partial}{\partial z} (\mathbf{V} \cdot \nabla_3 \Theta) dV + \int_{\mathcal{V}} \Theta_z q_z dV \\
&= -(\sigma Re)^{-1} \int_{\mathcal{V}} |\nabla_3 \Theta_z|^2 dV - \int_{\mathcal{V}} \mathbf{V} \cdot \nabla_3 (\tfrac{1}{2} \Theta_z^2) dV \\
&- \int_{\mathcal{V}} \Theta_z (u_z \Theta_x + v_z \Theta_y + \varepsilon w_z \Theta_z) dV + \int_{\mathcal{V}} \Theta_z q_z dV. \quad (3.45)
\end{aligned}$$

However, given that $\operatorname{div} bV = 0$ and $w = 0$ on S^\pm

$$\begin{aligned}
\int_{\mathcal{V}} \mathbf{V} \cdot \nabla_3 (\tfrac{1}{2} \Theta_z^2) dV &= \int_{\mathcal{V}} \{ \operatorname{div} (\tfrac{1}{2} \Theta_z^2 \mathbf{V}) - \tfrac{1}{2} \Theta_z^2 \operatorname{div} \mathbf{V} \} dV \\
&= \tfrac{1}{2} \int_S (\hat{\mathbf{n}} \cdot \mathbf{V}) \Theta_z^2 dS \\
&= \pm \tfrac{1}{2} \varepsilon \int_{S^\pm} w \Theta_z^2 dx dy = 0. \quad (3.46)
\end{aligned}$$

Integrating by parts the 3rd and 4th terms in (3.45) gives

$$\begin{aligned}
\frac{1}{2} \frac{d}{dt} \int_{\mathcal{V}} |\Theta_z|^2 dV &= -(\sigma Re)^{-1} \int_{\mathcal{V}} |\nabla_3 \Theta_z|^2 dV + \int_{\mathcal{V}} \Theta_z (u_{xz} + v_{yz} + \varepsilon w_{zz}) \Theta dV \\
&+ \int_{\mathcal{V}} \Theta (u_z \Theta_{xz} + v_z \Theta_{yz} + \varepsilon w_z \Theta_{zz}) dV - \int_{\mathcal{V}} \Theta_{zz} q dV \\
&= -(\sigma Re)^{-1} \int_{\mathcal{V}} |\nabla_3 \Theta_z|^2 dV + \int_{\mathcal{V}} \Theta (u_z \Theta_{xz} + v_z \Theta_{yz} + \varepsilon w_z \Theta_{zz}) dV \\
&- \int_{\mathcal{V}} \Theta_{zz} q dV \quad (3.47)
\end{aligned}$$

where $\operatorname{div} \mathbf{V} = 0$ has been used. Using inequality (B.6) in Appendix B, we find

$$\begin{aligned} \frac{1}{2} \frac{d}{dt} \int_{\mathcal{V}} |\Theta_z|^2 dV &\leq -(\sigma Re)^{-1} \int_{\mathcal{V}} |\nabla_3 \Theta_z|^2 dV + \|\Theta_{zz}\|_2 \|q\|_2 \\ &+ \|\Theta\|_6 \{ \|u_z\|_3 \|\Theta_{xz}\|_2 + \|v_z\|_3 \|\Theta_{yz}\|_2 + \varepsilon \|w_z\|_3 \|\Theta_{zz}\|_2 \}. \end{aligned} \quad (3.48)$$

Lemma 4 in Appendix C allows $\|u_z\|_3$, $\|v_z\|_3$ and $\|w_z\|_3$ to be estimated in terms of their second derivatives. Multiplying by Re^γ , where γ is to be determined, (3.48) becomes

$$\begin{aligned} \frac{1}{2} \frac{d}{dt} Re^\gamma \int_{\mathcal{V}} |\Theta_z|^2 dV &\leq -(\sigma Re)^{-1} Re^\gamma \int_{\mathcal{V}} |\nabla_3 \Theta_z|^2 dV + 2^{1/2} \varepsilon Re^\gamma \|\Theta\|_6 \|w\|_6^{1/2} \|w_{zz}\|_2^{1/2} \|\Theta_{zz}\|_2 \\ &+ Re^\gamma \{ 6^{1/2} \|v_{zz}\|_2^{1/2} \|v\|_6^{1/2} + 3^{1/3} \|v\|_2^{1/3} \|s\|_4^{2/3} \} \|\Theta\|_6 \{ \|\Theta_{xz}\|_2 + \|\Theta_{yz}\|_2 \} \\ &+ Re^\gamma \|\Theta_{zz}\|_2 \|q\|_2. \end{aligned} \quad (3.49)$$

In turn, this re-arranges to

$$\begin{aligned} \frac{1}{2} Re^\gamma \frac{d}{dt} \int_{\mathcal{V}} |\Theta_z|^2 dV &\leq -(\sigma Re)^{-1} Re^\gamma \int_{\mathcal{V}} |\nabla_3 \Theta_z|^2 dV \\ &+ [4\delta_3 Re^{-1} \varepsilon^2 \|w_{zz}\|_2^2]^{1/4} [\delta_3 (\sigma Re)^{-1} Re^\gamma \|\Theta_{zz}\|_2^2]^{1/2} \\ &\times [\delta_3^{-3} \sigma^2 Re^{b_1} \|\Theta\|_6^6]^{1/6} [\delta_3^{-3} \varepsilon^6 \sigma^2 Re^{b_2} \|w\|_6^6]^{1/12} \\ &+ \{ [4\delta_4 Re^{-1} \|v_{zz}\|_2^2]^{1/4} [3^6 \delta_4^{-3} Re^{c_2} \|v\|_6^6]^{1/12} \\ &+ [3\varepsilon^{-2} Re \|v\|_2^2]^{1/6} [3Re^{-1} \varepsilon^2 \|s\|_4^4]^{1/6} \} \\ &\times \left[\frac{\sigma^3}{8\delta_4^3} Re^{c_1} \|T\|_6^6 \right]^{1/6} \{ 2\delta_4 (\sigma Re)^{-1} Re^\gamma [\|\Theta_{xz}\|_2^2 + \|\Theta_{yz}\|_2^2] \}^{1/2} \\ &+ \{ \delta_5 (\sigma Re)^{-1} Re^\gamma \|\Theta_{zz}\|_2^2 \}^{1/2} \{ \delta_5^{-1} (\sigma Re) Re^\gamma \|q\|_2^2 \}^{1/2}. \end{aligned} \quad (3.50)$$

where $2b_1 + b_2 = 9 + 6\gamma$ and $2c_1 + c_2 = 9 + 6\gamma$. Using Young's inequality as in (B.7) in Appendix B, we obtain

$$\begin{aligned} \frac{1}{2} Re^\gamma \frac{d}{dt} \int_{\mathcal{V}} |\Theta_z|^2 dV &\leq -(\sigma Re)^{-1} Re^\gamma \int_{\mathcal{V}} |\nabla_3 \Theta_z|^2 dV \\ &+ \delta_3 Re^{-1} \varepsilon^2 \|w_{zz}\|_2^2 + \frac{1}{2} \delta_3 (\sigma Re)^{-1} Re^\gamma \|\Theta_{zz}\|_2^2 \\ &+ \frac{1}{6} \delta_3^{-3} \sigma^2 Re^{b_1} \|\Theta\|_6^6 + \frac{1}{12} \delta_3^{-3} \varepsilon^6 \sigma^2 Re^{b_2} \|w\|_6^6 \\ &+ \delta_4 Re^{-1} \|v_{zz}\|_2^2 + \delta_4 (\sigma Re)^{-1} Re^\gamma [\|\Theta_{xz}\|_2^2 + \|\Theta_{yz}\|_2^2] \\ &+ \frac{1}{48\delta_4^3} \sigma^3 Re^{c_1} \|\Theta\|_6^6 + \frac{3^6}{12\delta_4^3} Re^{c_2} \|v\|_6^6 + \frac{1}{2\varepsilon^2} Re \|v\|_2^2 + \frac{\varepsilon^2}{2} Re^{-1} \|s\|_4^4 \\ &+ \frac{1}{2} \delta_5 (\sigma Re)^{-1} Re^\gamma \|\Theta_{zz}\|_2^2 + \frac{1}{2} \delta_5^{-1} (\sigma Re) Re^\gamma \|q\|_2^2 \end{aligned} \quad (3.51)$$

Gathering terms we find

$$\begin{aligned}
\frac{1}{2}Re^\gamma \frac{d}{dt} \int_{\mathcal{V}} |\Theta_z|^2 dV &\leq -(\sigma Re)^{-1} Re^\gamma \int_{\mathcal{V}} \left\{ (1 - \delta_4)(|\Theta_{xz}|^2 + |\Theta_{yz}|^2) + (1 - \frac{1}{2}\delta_3 - \frac{1}{2}\delta_5)|\Theta_{zz}|^2 \right\} dV \\
&+ Re^{-1} \left\{ \delta_4 \|\mathbf{v}_{zz}\|_2^2 + \delta_3 \varepsilon^2 \|w_{zz}\|_2^2 \right\} + \frac{3^6}{12\delta_4^3} Re^{c_2} \|\mathbf{v}\|_6^6 \\
&+ \left\{ \frac{\sigma^2}{6\delta_3^3} Re^{b_1} + \frac{\sigma^3}{48\delta_4^3} Re^{c_1} \right\} \|\Theta\|_6^6 + \frac{\varepsilon^6 \sigma^2}{12\delta_3^3} Re^{b_2} \|w\|_6^6 \\
&+ \frac{1}{2}\delta_5^{-1} (\sigma Re) Re^\gamma \|q\|_2^2 + \frac{1}{2\varepsilon^2} Re \|\mathbf{v}\|_2^2 + \frac{\varepsilon^2}{2} Re^{-1} \|\mathbf{s}\|_4^4
\end{aligned} \tag{3.52}$$

3.3 Combination of the fluid and temperature inequalities

(3.52) is now combined with (3.33)

$$\begin{aligned}
\frac{1}{2} \frac{d}{dt} \int_{\mathcal{V}} |\zeta|^2 dV &+ \frac{1}{2} Re^\gamma \frac{d}{dt} \int_{\mathcal{V}} |\Theta_z|^2 dV \\
&\leq -\left(1 - \frac{3}{2}\delta_1 - 2\delta_2\right) Re^{-1} \int_{\mathcal{V}} |\text{curl } \zeta|^2 dV \\
&- (\sigma Re)^{-1} Re^\gamma \int_{\mathcal{V}} \left\{ (1 - \delta_4)(|\Theta_{xz}|^2 + |\Theta_{yz}|^2) + (1 - \frac{1}{2}\delta_3 - \frac{1}{2}\delta_5)|\Theta_{zz}|^2 \right\} dV \\
&+ Re^{-1} \left\{ \delta_4 \|\mathbf{v}_{zz}\|_2^2 + \delta_3 \varepsilon^2 \|w_{zz}\|_2^2 \right\} + \left(\frac{20}{3\delta_1^3} Re^3 + \frac{3^6}{12\delta_4^3} Re^{c_2} \right) \|\mathbf{v}\|_6^6 \\
&+ \varepsilon^6 \left(\frac{10}{3\delta_1^3} Re^3 + \frac{\sigma^2}{12\delta_3^3} Re^{b_2} \right) \|w\|_6^6 + \left(\frac{\sigma^2}{6\delta_3^3} Re^{b_1} + \frac{\sigma^3}{48\delta_4^3} Re^{c_1} \right) \|\Theta\|_6^6 \\
&+ \frac{1}{\varepsilon^2} \left(\frac{1}{2} + \delta_2 + \frac{1}{2\delta_2} \right) Re \|\mathbf{v}\|_2^2 + \frac{a_0^2}{2\varepsilon^2 \delta_2} Re \|\Theta\|_2^2 + \frac{1}{2}\delta_5^{-1} (\sigma Re) Re^\gamma \|q\|_2^2 \\
&+ \left(\frac{3}{2}\delta_1 + \frac{1}{2\delta_2} \right) Re^{-1} \|\mathbf{s}\|_2^2 + \frac{1}{2}\varepsilon^2 Re^{-1} \|\mathbf{s}\|_4^4
\end{aligned} \tag{3.53}$$

and

$$\left. \begin{aligned} 2b_1 + b_2 \\ 2c_1 + c_2 \end{aligned} \right\} = 9 + 6\gamma \tag{3.54}$$

Our choices are

$$b_1 = c_1 = -3, \quad b_2 = c_2 = 3, \quad \gamma = -2. \tag{3.55}$$

δ_3 and δ_4 also need to be chosen such that the $\|\mathbf{v}_{zz}\|_2^2$ - and $\varepsilon^2 \|w_{zz}\|_2^2$ -terms cancel from $\|\text{curl } \zeta\|_2^2$. To this end we choose $\delta_0 = \frac{1}{2}$ and make

$$\begin{aligned} 1 - \frac{3}{2}\delta_1 - 2\delta_2 &= \delta_4 \\ (1 - \frac{3}{2}\delta_1 - 2\delta_2)(1 - \delta_0) &= \delta_3. \end{aligned} \tag{3.56}$$

Hence $\delta_4 = 2\delta_3$. With this we choose δ_5 such that the coefficients $1 - \delta_4$ and $1 - \frac{1}{2}\delta_3 - \frac{1}{2}\delta_5$ within the double derivatives of the temperature are equal. Thus $\delta_5 = 3\delta_3$. Together we have

$$\delta_3 = \frac{1}{2} \left(1 - \frac{3}{2}\delta_1 - \frac{1}{2}\delta_2 \right), \quad \delta_4 = 2\delta_3, \quad \delta_5 = 3\delta_3. \tag{3.57}$$

where δ_1 and δ_2 are arbitrarily chosen under the constraint that $\delta_3 > 0$.

Now we turn to the last three steps in the calculation:

Step 1: To deal with the first set of terms on the right hand side of (3.53) we use the expression for $\|\text{curl } \boldsymbol{\zeta}\|_2^2$ in Lemma 3 with $\delta_0 = \frac{1}{2}$ and write

$$\int_{\mathcal{V}} |\text{curl } \boldsymbol{\zeta}|^2 dV - \left(\|\mathbf{v}_{zz}\|_2^2 + \frac{1}{2}\varepsilon^2 \|w_{zz}\|_2^2 \right) = \int_{\mathcal{V}} \{|\nabla_3 \omega_3|^2 + |u_{yz}|^2 + |v_{xz}|^2\} dV \quad (3.58)$$

This turns (3.53) into

$$\begin{aligned} \frac{1}{2} \frac{d}{dt} \int_{\mathcal{V}} |\boldsymbol{\zeta}|^2 dV &+ \frac{1}{2} Re^{-2} \frac{d}{dt} \int_{\mathcal{V}} |\Theta_z|^2 dV \\ &\leq -2\delta_3 Re^{-1} \int_{\mathcal{V}} \{|\nabla_3 \omega_3|^2 + |u_{yz}|^2 + |v_{xz}|^2\} dV \\ &- \sigma^{-1} (1 - 2\delta_3) Re^{-3} \int_{\mathcal{V}} |\nabla_3 \Theta_z|^2 dV + \left(\frac{20}{3\delta_1^3} + \frac{243}{32\delta_3^3} \right) Re^3 \|\mathbf{v}\|_6^6 \\ &+ \varepsilon^6 \left(\frac{10}{3\delta_1^3} + \frac{\sigma^2}{12\delta_3^3} \right) Re^3 \|w\|_6^6 + \frac{\sigma^2}{6\delta_3^3} \left(1 + \frac{\sigma}{64} \right) Re^{-3} \|\Theta\|_6^6 \\ &+ \varepsilon^{-2} Re \left[\left(\frac{1}{2} + \delta_2 + \frac{1}{2\delta_2} \right) \|\mathbf{v}\|_2^2 + \frac{a_0^2}{2\delta_2} \|\Theta\|_2^2 \right] + \frac{\sigma}{6\delta_3} Re^{-1} \|q\|_2^2 \\ &+ \left(\frac{3}{2}\delta_1 + \frac{1}{2\delta_2} \right) Re^{-1} \|\mathbf{s}\|_2^2 + \frac{1}{2}\varepsilon^2 Re^{-1} \|\mathbf{s}\|_4^4 + \frac{1}{2} Re^{-1} G_{S^+}(\omega_3, \mathbf{s}). \end{aligned} \quad (3.59)$$

Step 2: Now we re-scale back to dimensional variables defined in Table 2 and $\mathcal{H}(t)$ defined in (2.4). This involves multiplying both sides of (3.59) by Re^3 .

$$\begin{aligned} \frac{1}{2} \frac{d\mathcal{H}}{dt} &\leq -\frac{2\delta_3 L^2}{\omega_0^2} \int_{\mathcal{V}} (|\nabla_3 \Omega_3|^2 + \alpha_a^2 |u_{1,x_2x_3}|^2 + \alpha_a^2 |u_{2,x_1x_3}|^2) dV - \frac{(1 - 2\delta_3)L^4}{\sigma T_0^2} \int_{\mathcal{V}} |\nabla T_{x_3}|^2 dV \\ &+ \left(\frac{20}{3\delta_1^3} + \frac{243}{32\delta_3^3} \right) \|\mathcal{R}_{u_{hor}}\|_6^6 + \left(\frac{10}{3\delta_1^3} + \frac{\sigma^2}{12\delta_3^3} \right) \|\mathcal{R}_{u_3}\|_6^6 + \frac{\alpha_a^{-6} \sigma^2}{6\delta_3^3} \left(1 + \frac{\sigma}{64} \right) \|\mathcal{R}_{a,T}\|_6^6 \\ &+ \varepsilon^{-2} \left\{ \left(\frac{1}{2} + \delta_2 + \frac{1}{2\delta_2} \right) Re^2 \|\mathcal{R}_{u_1}\|_2^2 + \frac{a_0^2 \alpha_a^{-6}}{2\delta_2} Re^4 \|\mathcal{R}_{a,T}\|_2^2 \right\} + \frac{\sigma}{6\delta_3} Re \|q\|_2^2 \\ &+ \left(\frac{3}{2}\delta_1 + \frac{1}{2\delta_2} \right) Re^2 \|\mathbf{S}\|_2^2 + \frac{1}{2}\varepsilon^2 \omega_0^{-2} Re^2 \|\mathbf{S}\|_4^4 + \frac{L^{-1}}{2\omega_0^2} \int_{\mathcal{V}} G_{S^+}(\Omega_3, \mathbf{S}) dV. \end{aligned} \quad (3.60)$$

Step 3: Finally, we take the time integral over an interval $[0, \tau_*]$.

$$\begin{aligned} \int_0^{\tau_*} \int_{\mathcal{V}} \left\{ -\frac{2\delta_3 L^2}{\omega_0^2} \{|\nabla_3 \Omega_3|^2 + \alpha_a^2 |u_{1,x_2x_3}|^2 + \alpha_a^2 |u_{2,x_1x_3}|^2\} - \frac{(1 - 2\delta_3)L^4}{\sigma T_0^2} |\nabla T_{x_3}|^2 \right. \\ \left. + \beta_{u_{hor}} |\mathcal{R}_{u_{hor}}|^6 + \beta_{u_3} |\mathcal{R}_{u_3}|^6 + \beta_{1,T} |\mathcal{R}_{a,T}|^6 + \beta_{2,T} Re^4 \mathcal{R}_{a,T}^2 + F_H(Q, \mathbf{S}) \right. \\ \left. + \frac{1}{2} \mathcal{V}_*^{-1} \mathcal{H}(0) \right\} dV dt \geq \frac{1}{2} \mathcal{H}(\tau_*). \end{aligned} \quad (3.61)$$

Because of regularity [29, 30, 31, 32] $\mathcal{H}(\tau_*)$ is always under control from above and it also has a uniform lower bound $\mathcal{H}(\tau_*) > 0$ although zero may be a poor lower bound.

Together with the use of Lemma 3 with $\delta_0 = \frac{1}{2}$, gives the result of Theorem 1, where $\beta_{u_{hor}}$, β_{u_3} and $\beta_{i,T}$ are defined in Table 3 and the forcing function $F_H(Q, \mathbf{S})$ is defined in (2.2).

■

4 Proof of (non-hydrostatic) Theorem 2

(1.11) for the non-hydrostatic case is

$$\varepsilon \left(\frac{\partial}{\partial t} + \mathbf{V} \cdot \nabla_3 \right) \mathbf{v} + \mathbf{k} \times \mathbf{v} + a_0 \mathbf{k} \Theta = \varepsilon Re^{-1} \Delta_3 \mathbf{v} - \nabla_3 p. \quad (4.1)$$

with the equation for the temperature remaining as in (1.9). Appendix B shows that

$$- \mathbf{V} \cdot \nabla_3 \mathbf{v} = \mathbf{V} \times \mathbf{w} - \frac{1}{2} \nabla_3 [u_3^2 - \varepsilon^2 w^2 (\alpha_a^2 - 1)^2], \quad (4.2)$$

so the curl-operation on (4.1) gives

$$\varepsilon \frac{\partial \mathbf{w}}{\partial t} = \varepsilon Re^{-1} \Delta_3 \mathbf{w} + \varepsilon \operatorname{curl} (\mathbf{V} \times \mathbf{w}) - \operatorname{curl} (\mathbf{k} \times \mathbf{v} + a_0 \mathbf{k} \Theta) \quad (4.3)$$

without involving pressure terms. The differential inequalities for $\int_{\mathcal{V}} |\mathbf{w}|^2 dV$ and $\int_{\mathcal{V}} |\Theta_z|^2 dV$ in the non-hydrostatic case are computed in the same manner as before but with periodic boundary conditions; this eliminates the terms in $\|\mathbf{s}\|_2$ and $\|\mathbf{s}\|_4$ with changes in the arithmetic of the coefficients. For this reason we leave out most of the working and express the results with the arbitrary constants δ_i of §3 replaced by η_i . Integrating by parts on periodic boundary conditions gives

$$\begin{aligned} \frac{1}{2} \varepsilon \frac{d}{dt} \int_{\mathcal{V}} |\mathbf{w}|^2 dV &= -\varepsilon Re^{-1} \int_{\mathcal{V}} |\operatorname{curl} \mathbf{w}|^2 dV + \varepsilon \int_{\mathcal{V}} (\operatorname{curl} \mathbf{w}) \cdot (\mathbf{V} \times \mathbf{w}) dV \\ &\quad - \int_{\mathcal{V}} (\operatorname{curl} \mathbf{w}) \cdot (\mathbf{k} \times \mathbf{v} + a_0 \mathbf{k} \Theta) dV, \end{aligned} \quad (4.4)$$

from which, for arbitrary $\eta_1, \eta_2 > 0$, we find

$$\begin{aligned} \frac{1}{2} \frac{d}{dt} \int_{\mathcal{V}} |\mathbf{w}|^2 dV &\leq - (1 - \frac{3}{4} \eta_1 - \eta_2) Re^{-1} \int_{\mathcal{V}} |\operatorname{curl} \mathbf{w}|^2 dV \\ &\quad + \frac{2Re^3}{\eta_1^3} \|\mathbf{v}\|_6^6 + \frac{Re^3 \varepsilon^6 \alpha_a^{12}}{\eta_1^3} \|w\|_6^6 + \frac{Re}{2\varepsilon^2 \eta_2} (\|\mathbf{v}\|_2^2 + a_0^2 \|\Theta\|_2^2). \end{aligned} \quad (4.5)$$

The estimate for the temperature field, equivalent to (3.52) is

$$\begin{aligned} \frac{1}{2} Re^{-2} \frac{d}{dt} \int_{\mathcal{V}} |\Theta_z|^2 dV &\leq -\sigma^{-1} Re^{-3} \int_{\mathcal{V}} \left\{ (1 - \eta_4) (|\Theta_{xz}|^2 + |\Theta_{yz}|^2) + (1 - \frac{1}{2} \eta_3 - \frac{1}{2} \eta_5) |\Theta_{zz}|^2 \right\} dV \\ &\quad + Re^{-1} \left\{ \eta_4 \|\mathbf{v}_{zz}\|_2^2 + \eta_3 \varepsilon^2 \alpha_a^4 \|w_{zz}\|_2^2 \right\} + \frac{3^6}{12\eta_4^3} Re^3 \|\mathbf{v}\|_6^6 \\ &\quad + Re^{-3} \left\{ \frac{\sigma^2}{6\eta_3^3} + \frac{\sigma^3}{48\eta_4^3} \right\} \|\Theta\|_6^6 + \frac{\varepsilon^6 \alpha_a^{12} \sigma^2}{12\eta_3^3} Re^3 \|w\|_6^6 + \frac{1}{2} \eta_5^{-1} \sigma Re^{-1} \|q\|_2^2. \end{aligned} \quad (4.6)$$

With $1 - \eta_4 = 1 - \frac{1}{2}\eta_3 - \frac{1}{2}\eta_5$ together (4.5) and (4.6) become

$$\begin{aligned}
\frac{1}{2} \frac{d}{dt} \int_{\mathcal{V}} (|\mathbf{w}|^2 dV + Re^{-2} |\Theta_z|^2) dV &\leq - (1 - \frac{3}{4}\eta_1 - \eta_2) Re^{-1} \int_{\mathcal{V}} |\operatorname{curl} \mathbf{w}|^2 dV \\
&- \sigma^{-1} (1 - \eta_4) Re^{-3} \int_{\mathcal{V}} |\nabla \Theta_z|^2 dV \\
&+ Re^{-1} \{ \eta_4 \| \mathbf{v}_{zz} \|_2^2 + \eta_3 \varepsilon^2 \alpha_a^4 \| w_{zz} \|_2^2 \} \\
&+ Re^3 \left[\frac{2}{\eta_1^3} + \frac{3^6}{12\eta_4^3} \right] \| \mathbf{v} \|_6^6 + Re^3 \varepsilon^6 \alpha_a^{12} \left(\frac{\sigma^2}{12\eta_3^3} + \frac{1}{\eta_1^3} \right) \| w \|_6^6 \\
&+ Re^{-3} \left\{ \frac{\sigma^2}{6\eta_3^3} + \frac{\sigma^3}{48\eta_4^3} \right\} \| \Theta \|_6^6 \\
&+ \frac{Re}{2\varepsilon^2 \eta_2} (\| \mathbf{v} \|_2^2 + a_0^2 \| \Theta \|_2^2) + \frac{1}{2} \eta_5^{-1} \sigma Re^{-1} \| q \|_2^2
\end{aligned} \tag{4.7}$$

Thus with the choice $\eta_3 = \eta_4 = \eta_5 = \frac{1}{4}\eta_1$ together with the fact that

$$\| \mathbf{v}_{zz} \|_2^2 + \varepsilon^2 \alpha_a^4 \| w_{zz} \|_2^2 \leq \| \operatorname{curl} \mathbf{w} \|_2^2 \tag{4.8}$$

(4.7) becomes

$$\begin{aligned}
\frac{1}{2} \frac{d}{dt} \int_{\mathcal{V}} (|\mathbf{w}|^2 dV + Re^{-2} |\Theta_z|^2) dV &\leq - (1 - \eta_1 - \eta_2) Re^{-1} \int_{\mathcal{V}} |\operatorname{curl} \mathbf{w}|^2 dV \\
&- \sigma^{-1} (1 - \frac{1}{4}\eta_1) Re^{-3} \int_{\mathcal{V}} |\nabla \Theta_z|^2 dV \\
&+ \frac{64}{\eta_1^3} Re^3 \left[2 + \frac{3^6}{12} \right] \| \mathbf{v} \|_6^6 + \frac{\varepsilon^6 \alpha_a^{12}}{\eta_1^3} \left(\frac{\sigma^2}{12} + 1 \right) Re^3 \| w \|_6^6 \\
&+ \frac{64}{\eta_1^3} Re^{-3} \left\{ \frac{\sigma^2}{6} + \frac{\sigma^3}{48} \right\} \| \Theta \|_6^6 \\
&+ \frac{Re}{2\varepsilon^2 \eta_2} (\| \mathbf{v} \|_2^2 + a_0^2 \| \Theta \|_2^2) + \frac{2\sigma}{\eta_1} Re^{-1} \| q \|_2^2
\end{aligned} \tag{4.9}$$

Re-dimensionalizing as in (2.5) in Theorem 1 and using $\mathcal{N}(t)$ defined in (2.9) we end up with (2.10) in Theorem 2. The assumption of regularity is necessary on two counts: (i) for arbitrary values of τ_* bounded-ness from above of $\mathcal{N}(\tau_*)$ is required; (ii) for the extraction of solutions point-wise from the space-time integral. The uniform lower bound $\mathcal{N}(\tau_*) > 0$ is also used. \blacksquare

5 Potential implications for simulations

Much of this article has been written with the hope of dual usage in both atmospheric and oceanic contexts. However, the boundary conditions are quite different in the two cases. The cylinder boundary conditions used by Cao and Titi [29, 30] are consistent with the oceanic context. In the atmosphere, the fixed upper lid condition used here could conceivably be applied at the tropopause instead of imposing a radiation condition. An imposed drag at the bottom of the domain could also be easily adopted. However, the complex physics of the planetary boundary layer of the atmosphere must be ignored in our formulation. In any case we believe that the

conclusions will not be seriously altered by a change in boundary conditions. The HPE and NPE can develop extremely small scales of motion, allowed by the estimates given here. These size scales decrease as \mathcal{R}_u^{-1} , \mathcal{R}_w^{-1} and $\mathcal{R}_{a,T}^{-1}$, which means they could easily become of the order of metres or less at the very large values of these parameters achieved in both atmospheric and oceanic flows. The importance of the tendency to produce vigorous intermittent small scales in NWP and ocean circulation simulations remains to be determined. This tendency may effect parameterizations as numerical resolution improves. In particular, one may ask whether parameterizations developed at coarser scales will still be accurate at finer scales, if the finer scales undergo the extreme events whose potential appearance has been predicted in this paper. As for the perennial question of initial conditions, one must hope that flow activity initialized at coarse scales will be consistently followed to smaller scales without undue amplification of simulation errors.

In the two Theorems in §2, space-time divided into two distinct regions \mathbb{S}^+ and \mathbb{S}^- . The region \mathbb{S}^- could be a union of a large number of disjoint sets, and if it were non-empty the flows in \mathbb{S}^- would be dominated by strong concentrated structures. Very large lower bounds on double mixed derivatives of components of the velocity field (u_1, u_2, u_3) such as $|\partial^2 u_1 / \partial x_3 \partial x_2|^2$ or $|\partial^2 u_2 / \partial x_1 \partial x_3|^2$ occur within \mathbb{S}^- : these represent intense accumulation in the (x_1, x_3) - and (x_2, x_3) -planes respectively. Thus, for a nonempty \mathbb{S}^- , one would see the spontaneously formation of front-like objects localised in space that would only exist for a finite time. $\mathcal{R}_{u_{hor}}$ and \mathcal{R}_{u_3} are *local* Reynolds numbers depending upon the local space-time values of $u(x_1, x_2, x_3, \tau) = \sqrt{u_1^2 + u_2^2}$ and the vertical velocity $u_3 = u_3(x_1, x_2, x_3, \tau)$ and $\mathcal{R}_{a,T}$ is a Rayleigh number dependent on the local temperature $T(x_1, x_2, x_3, \tau)$. In both the hydrostatic and non-hydrostatic cases the large lower bounds on double-derivatives of solutions within the \mathbb{S}^- regions can be converted into the large lower bounds on inverse length scales $\lambda_{H,N}^{-1}$ given in (2.13). Thus to resolve a region such as this would require

$$\text{Number of grid points} > \text{const} (\mathcal{R}_{u_{hor}}^3 + \mathcal{R}_{u_3}^3 + \mathcal{R}_{a,T}^3 + Re^2 \mathcal{R}_{a,T}). \quad (5.1)$$

It is also worth remarking that the L^6 -norm arising in the proofs of Theorems 3 and 4, and leading to the sixth powers of the *local* Reynolds numbers $\mathcal{R}_{u_{hor}}$ and \mathcal{R}_{u_3} for $\lambda_{H,N}^{-1}$, is precisely the norm that was proved by Cao and Titi [29, 30] to be bounded for HPE. While $\mathcal{R}_{u_{hor}}$ and \mathcal{R}_{u_3} are functions of space-time they are bounded functions, but what is not known is how much $\mathcal{R}_{u_{hor}}$ (say) oscillates around its global space-time average Re . It may be significantly smaller or larger in various parts of the flow. Thus, how $\mathbf{u}_3 = \{u_1, u_2, u_3\}$ varies across a front is an important issue. The limitations of the result are that no further information is available from the analysis regarding the spatial or temporal statistics of the subsets of \mathbb{S}^- on which intense events would occur.

The results for the HPE and NPE cases are qualitatively the same although there are also significant differences. The main differences are that regularity of solutions of the NPE needs to be assumed, and the domain needs to be made periodic in the velocity variables and their derivatives. The temperature boundary conditions remain identical. In the hydrostatic case \mathcal{R}_{u_3}

is expected to be negligible compared to $\mathcal{R}_{u_{hor}}$, but in the non-hydrostatic case its contribution may be significant in regions of strong vertical convection. The hydrostatic estimates for the two length scales defined $\lambda_{H,N}$ in (2.11) and (2.12) is of the order of a *metre* or less. Of course, this very small estimate may not be the thickness of a front; instead, it may refer to the smallest scale of features *within* a front.

Future improvements in numerical capabilities for the prediction of weather, climate and ocean circulation may be expected to enhance spatial and temporal resolutions. In addition, they will raise the issue of the optimal allocation of numerical resources. For example, improving the computations for parameterizations of other currently unresolved physical processes (such as phase changes in cloud physics) may have effects that are at least as significant as computing non-hydrostatic effects at finer resolution. Improvements in resolution will also raise the issue of whether subgrid-scale parameterizations of these unresolved physical processes that have been developed for numerical prediction at coarser scales will transfer accurately to computations at finer scales, regardless of whether the hydrostatic approximation is retained. Thus, one may expect the HPE to remain central in the discussions about choices among the various potential numerical code implementations for weather, climate and ocean circulation predictions well into the foreseeable future. Even though they are mathematically well-posed, the HPE were shown here to contain the potential for sudden, localized events to occur on extremely small scales in space and time. The NPE have this same capability, but their well-posedness remains in question.

Acknowledgements: We thank Peter Bartello, Mike Cullen, Raymond Hide, Brian Hoskins, Peter Lynch, Tim Palmer, Ian Roulstone, Edriss Titi and Andy White for several enlightening conversations. Darryl Holm thanks the Royal Society for a Wolfson Research Merit Award.

A Appendix A: Relations between $\boldsymbol{\omega}$, $\boldsymbol{\zeta}$ and \boldsymbol{w}

With $\boldsymbol{v} = (u, v, 0)$ and $\boldsymbol{V} = (u, v, \varepsilon w)$ we know that the full vorticity $\boldsymbol{\omega} = \text{curl } \boldsymbol{V}$ is given by

$$\boldsymbol{\omega} = \boldsymbol{i}(\varepsilon w_y - v_z) - \boldsymbol{j}(\varepsilon w_x - u_z) + \boldsymbol{k}(v_z - u_y) \quad (\text{A.1})$$

This is related to $\boldsymbol{\zeta} = \text{curl } \boldsymbol{v}$ by

$$\boldsymbol{\zeta} = \boldsymbol{\omega} + \varepsilon \nabla^\perp w \quad (\text{A.2})$$

where $\nabla^\perp = -\boldsymbol{i}\partial_y + \boldsymbol{j}\partial_x$. Therefore we have

$$\boldsymbol{V} \times \boldsymbol{\omega} = \boldsymbol{V} \times (\boldsymbol{\zeta} - \varepsilon \nabla^\perp w) \quad (\text{A.3})$$

and so

$$\begin{aligned} \boldsymbol{V} \times \boldsymbol{\zeta} &= -\boldsymbol{V} \cdot \nabla_3 \boldsymbol{V} + \nabla_3 \left(\frac{1}{2} u_3^2 \right) + \varepsilon \boldsymbol{V} \times \nabla^\perp w \\ &= -\boldsymbol{V} \cdot \nabla_3 \boldsymbol{v} + \nabla_3 \left(\frac{1}{2} u_3^2 \right) + \varepsilon \boldsymbol{V} \times \nabla^\perp w - \varepsilon \boldsymbol{k} \boldsymbol{V} \cdot \nabla_3 w. \end{aligned} \quad (\text{A.4})$$

Thus

$$\mathbf{V} \times \boldsymbol{\zeta} + \mathbf{V} \cdot \nabla_3 \mathbf{v} - \nabla_3(\tfrac{1}{2}u_3^2) = \varepsilon \mathbf{V} \times \nabla^\perp w - \varepsilon \mathbf{k} \mathbf{V} \cdot \nabla_3 w. \quad (\text{A.5})$$

Moreover,

$$\begin{aligned} \mathbf{V} \times \nabla^\perp w &- \mathbf{k} \mathbf{V} \cdot \nabla_3 w \\ &= -\mathbf{k}(uw_x + vw_y + \varepsilon ww_z) - \mathbf{i}(\varepsilon ww_x) - \mathbf{j}(\varepsilon ww_y) + \mathbf{k}(uw_x + vw_y) \\ &= -\varepsilon w \nabla_3 w = -\varepsilon \nabla_3(\tfrac{1}{2}w^2). \end{aligned} \quad (\text{A.6})$$

Therefore, we have

$$\begin{aligned} -\mathbf{V} \cdot \nabla_3 \mathbf{v} &= \mathbf{V} \times \boldsymbol{\zeta} - \tfrac{1}{2} \nabla_3(u_3^2 - \varepsilon^2 w^2) \\ &= \mathbf{V} \times \boldsymbol{\zeta} - \tfrac{1}{2} \nabla_3(u^2 + v^2) \end{aligned} \quad (\text{A.7})$$

Finally, turning to $\mathbf{w} = \text{curl } \mathbf{v}$ for the non-hydrostatic case, we have

$$\mathbf{w} = \mathbf{i}(\varepsilon \alpha_a^2 w_y - v_z) - \mathbf{j}(\varepsilon \alpha_a^2 w_x - u_z) + \mathbf{k}(v_z - u_y) \quad (\text{A.8})$$

which shows that

$$\mathbf{w} = \boldsymbol{\omega} + \varepsilon(\alpha_a^2 - 1) \nabla^\perp w. \quad (\text{A.9})$$

Thus the result (A.7) found for \mathbf{v} , $\boldsymbol{\zeta}$ and $\boldsymbol{\omega}$ can be replicated with ε replaced by $\varepsilon(\alpha_a^2 - 1)$ together with \mathbf{v} by \mathbf{v} and $\boldsymbol{\zeta}$ by \mathbf{w} to give

$$-\mathbf{V} \cdot \nabla_3 \mathbf{v} = \mathbf{V} \times \mathbf{w} - \tfrac{1}{2} \nabla_3 [u_3^2 - \varepsilon^2 w^2 (\alpha_a^2 - 1)^2]. \quad (\text{A.10})$$

B Appendix B: Inequalities

The following standard inequalities have been used:

1. The standard inequality

$$|AB| \leq \tfrac{1}{2}|A|^2 + \tfrac{1}{2}|B|^2 \quad (\text{B.1})$$

using $|AB| = |\varepsilon A| |\varepsilon^{-1} B|$ can be modified to

$$|AB| \leq \frac{\varepsilon}{2}|A|^2 + \frac{1}{2\varepsilon}|B|^2 \quad (\text{B.2})$$

for any $\varepsilon > 0$. This often called *Young's inequality*.

2. For $\alpha, \beta, \gamma > 0$ and $\alpha + \beta + \gamma = 1$, one form of *Hölder's inequality* is

$$|A|^\alpha |B|^\beta |C|^\gamma \leq \alpha |A| + \beta |B| + \gamma |C| \quad (\text{B.3})$$

3. For $p, q, r > 0$ and $\frac{1}{p} + \frac{1}{q} + \frac{1}{r} = 1$, another form of Hölder's inequality under integration is:

$$\left| \int_{\mathcal{V}} ABC dV \right| \leq \left(\int_{\mathcal{V}} |A|^p dv \right)^{1/p} \left(\int_{\mathcal{V}} |B|^q dv \right)^{1/q} \left(\int_{\mathcal{V}} |C|^r dv \right)^{1/r} \quad (\text{B.4})$$

Now let's use the norm notation

$$\left(\int_{\mathcal{V}} |A|^p dv \right)^{1/p} \equiv \|A\|_p \quad (\text{B.5})$$

so (B.4) can be written as

$$\begin{aligned} \left| \int_{\mathcal{V}} ABC dV \right| &\leq \|A\|_p \|B\|_q \|C\|_r \\ &\leq \frac{1}{p} \|A\|_p^p + \frac{1}{q} \|B\|_q^q + \frac{1}{r} \|C\|_r^r \\ &= \int_{\mathcal{V}} \left(\frac{1}{p} |A|^p + \frac{1}{q} |B|^q + \frac{1}{r} |C|^r \right) dV \end{aligned} \quad (\text{B.6})$$

We could also have jumped to the last line using (B.3) directly with $\alpha = p^{-1}$ etc. One could also modify (B.6) according to Young's inequality in (B.2) and, for any $\epsilon > 0$ and $a + b + c = 0$, rewrite (B.6) as

$$\left| \int_{\mathcal{V}} ABC dV \right| \leq \frac{\epsilon^{ap}}{p} \|A\|_p^p + \frac{\epsilon^{bq}}{q} \|B\|_q^q + \frac{\epsilon^{cr}}{r} \|C\|_r^r. \quad (\text{B.7})$$

C Appendix C: Proof of the L^3 -Lemma

Lemma 4 *Given the Neumann boundary conditions on $C(H, L)$, the vector \mathbf{v}_z and the scalar w_z satisfy*

$$\|\mathbf{v}_z\|_3 \leq 6^{1/2} \|\mathbf{v}_{zz}\|_2^{1/2} \|\mathbf{v}\|_6^{1/2} + 3^{1/3} \|\mathbf{v}\|_2^{1/3} \|\mathbf{s}\|_4^{2/3}. \quad (\text{C.1})$$

$$\|w_z\|_3 \leq 2^{1/2} \|w_{zz}\|_2^{1/2} \|w\|_6^{1/2}. \quad (\text{C.2})$$

Proof:

$$\begin{aligned} \int_{\mathcal{V}} |\mathbf{v}_z|^3 dV &= \int_{\mathcal{V}} (|u_z|^2 + |v_z|^2)^{3/2} dV \\ &\leq \frac{3}{2} \int_{\mathcal{V}} (|u_z|^3 + |v_z|^3) dV \end{aligned} \quad (\text{C.3})$$

and, given the boundary conditions on u and v ,

$$\begin{aligned} \int_{\mathcal{V}} |u_z|^3 dV &= \int_{\mathcal{V}} u_z u_z |u_z| dV \\ &= - \int_{\mathcal{V}} \left\{ uu_{zz} |u_z| + uu_z \frac{d|u_z|}{dz} \right\} dV + \int_{S^\pm} uu_z |u_z| dx dy \\ &\leq 2 \int_{\mathcal{V}} |u| |u_{zz}| |u_z| dV + \int_{S^\pm} |u| |\mathbf{s}|^2 dx dy, \end{aligned} \quad (\text{C.4})$$

which holds because $d|f|/dz \leq |f_z|$ for any function f . Thus (C.3) becomes

$$\begin{aligned} \int_{\mathcal{V}} |\mathbf{v}_z|^3 dV &\leq 3 \int_{\mathcal{V}} \{|u| |u_{zz}| |u_z| + |v| |v_{zz}| |v_z|\} dV + \frac{3}{2} (\|u\|_2 + \|v\|_2) \|\mathbf{s}\|_4^2 \\ &\leq 6 \int_{\mathcal{V}} |\mathbf{v}| |\mathbf{v}_{zz}| |\mathbf{v}_z| dV + 3 \|\mathbf{v}\|_2 \|\mathbf{s}\|_4^2 \\ &\leq 6 \|\mathbf{v}\|_6 \|\mathbf{v}_{zz}\|_2 \|\mathbf{v}_z\|_3 + 3 \|\mathbf{v}\|_2 \|\mathbf{s}\|_4^2, \end{aligned} \quad (\text{C.5})$$

which gives the advertised result. The result for w follows in a similar manner. \square

References

- [1] Richardson L F (1922) *Weather Prediction by Numerical Process* (Cambridge: Cambridge University Press) reprinted by Dover New York (1988)
- [2] Charney J G (1955) The use of the primitive equations of motion in numerical prediction *Tellus* **7** 22–26
- [3] Eckart C. (1960) *The Hydrodynamics of Oceans and Atmospheres* (Oxford: Pergamon Press)
- [4] Gill A (1982) *Atmosphere-ocean dynamics* (London: Academic Press)
- [5] Pedlosky J (1987) *Geophysical Fluid Dynamics* 2nd edition (New York: Springer-Verlag)
- [6] Salmon R (1988) Hamiltonian fluid mechanics *Ann. Rev. Fluid Mech.* **20** 225–256
- [7] Holton J. R. (1992). *An Introduction to Dynamic Meteorology* 3rd edition (San Diego: Academic Press)
- [8] Cullen M J P (1993) The unified forecast/climate model *Meteorol. Mag.* **122** 81–94
- [9] Holm D D (1996) Hamiltonian balance equations *Physica D* **98** 379–414
- [10] Marshall J, Hill C, Perelman L and Adcroft A (1997) Hydrostatic, quasi-hydrostatic and non-hydrostatic ocean modelling *J. Geophys. Res.* **102** 5733–5752
- [11] Norbury J and Roulstone I (2002) *Large-scale atmosphere-ocean dynamics I & II* (Cambridge: Cambridge University Press)
- [12] White A A (2002) A view of the equations of meteorological dynamics and various approximations, in Norbury J and Roulstone I (eds) *Large-scale ocean-atmosphere dynamics I* (Cambridge: University Press)
- [13] White A A (2003) Primitive Equations in Holton J R *et al* (eds) *Encyclopedia of atmospheric science* (New York: Academic Press) pp. 694–702
- [14] Davies T, Cullen M J P, Malcolm A J, Mawson M H, Staniforth A, White A A and Wood N (2005) A new dynamical core for the Met Office’s global and regional modelling of the atmosphere *Q. J. R. Meteorol. Soc.* **131** 1759–1782
- [15] White A A, Hoskins B J, Roulstone I and Staniforth A (2005) Consistent approximate models of the global atmosphere: shallow, deep, hydrostatic, quasi-hydrostatic and non-hydrostatic *Q. J. R. Meteorol. Soc.* **131** 2081–2107

- [16] Cullen M J P (2006) *A Mathematical Theory of Large-scale Atmosphere/Ocean Flow* (London: Imperial College Press)
- [17] Cullen M J P (2007) Modelling Atmospheric Flows *Acta Numerica*, 1–87
- [18] Wedi N P and Smolarkiewicz P K (2009) A framework for testing global non-hydrostatic models *Q. J. R. Meteorol. Soc.* (Published online:DOI: 10.1002/qj)
- [19] Ohfuchi W, Sasaki H, Masumoto Y and Nakamura H (2005) Mesoscale resolving simulations of the global atmosphere and ocean on the Earth Simulator *EOS Trans. AGU* **86** 45–46
- [20] Shen B-W, Atlas R, Chern J-D, Reale O, Lin S-J, Lee T and Chang J (2006) The 0.125 degree finite-volume general circulation model on the NASA Columbia supercomputer: preliminary simulations of mesoscale vortices *Geophys. Res. Lett.* **33** L05801
- [21] Hamilton K, Takahashi Y O, and Ohfuchi W (2008) The mesoscale spectrum of atmospheric motions investigated in a very fine resolution global general circulation model. *J. Geophys. Res.* **113** D18110 doi:10.1029/2008JD009785
- [22] Eliassen A (1948) The quasi-static equations of motion *Geofys Publikasjoner* **17** No. 3
- [23] Hide R (1964) The viscous boundary layer at the free surface of a rotating baroclinic fluid *Tellus* **16** 523–529
- [24] Hide R (1965) The viscous boundary layer at the free surface of a rotating baroclinic fluid: effects due to the temperature dependence of surface tension *Tellus* **17** 440–442
- [25] Hide R (1969) Some laboratory experiments on free thermal convection in a rotating fluid subject to a horizontal temperature gradient and their relation to the global atmospheric circulation pp. 196-221 in *The Global Circulation of the Atmosphere* (ed. Corby G A) Royal Meteorological Society, London
- [26] Hoskins B J (1975) The Geostrophic momentum approximation and the semi-geostrophic equations *J. Atmos. Sci.* **32** 233–242
- [27] Hoskins B J and Bretherton F (1972) Atmospheric frontogenesis models; Mathematical formulation and solution *J. Atmos. Sci.* **29** 11–37
- [28] Hoskins B J (1982) The mathematical theory of frontogenesis *Ann. Rev. Fluid Mech.* **14** 131–151
- [29] Cao C and Titi E S (2005) *Global well-posedness of the three-dimensional primitive equations of large scale ocean and atmosphere dynamics* arXiv: Math. AP/0503028
- [30] Cao C and Titi E S (2007) Global well-posedness of the three-dimensional primitive equations of large scale ocean and atmosphere dynamics *Ann. Math.* **166** 245-267
- [31] Kobelkov G (2006) Existence of a solution “in whole” for the large-scale ocean dynamics equations *Comptes Rendus Acad. Sci. Paris I* **343** 283-286
- [32] Kobelkov G (2007) Existence of a Solution in the large for Ocean Dynamics Equations *J. Math. Fluid Mech.* **9** no. 4 588–610
- [33] Kobelkov G (2008) Existence and uniqueness of a solution to primitive equations with stratification in the large *Russian J. Numer. Anal. Math. Modelling* **23** 39–61

- [34] Ju N (2007) The global attractor for the solutions of the 3D viscous Primitive Equations Disc. Cont. Dyn. Systems **17** 159–179
- [35] Gibbon J D (2009) *Estimating intermittency in three-dimensional Navier-Stokes turbulence* J. Fluid Mechanics to appear
- [36] Raugel G and Sell G R (1993) Navier-Stokes equations on thin 3D domains. I. Global attractors and global regularity of solutions J. Amer. Math. Soc. **6** 503-568
- [37] Raugel G and Sell G R (1994) Navier-Stokes equations on thin 3D domains. II. Global regularity of spatially periodic solutions *Nonlinear partial differential equations and their applications* Collège de France Seminar Vol. XI (Harlow: Longman Sci. Tech.) pp 205-247
- [38] Hu C, Temam R and Ziane M (2003) The primitive equations on the large scale ocean under the small depth hypothesis Discrete Contin. Dynam. Systems **9** 97–131
- [39] Lions J Temam R and Wang S (1992) New formulations of the primitive equations of atmosphere and applications Nonlinearity **5** 237–288
- [40] Lions J Temam R and Wang S (1992) On the equations of the large scale Ocean Nonlinearity **5** 1007–1053
- [41] Lions J Temam R and Wang S (1995) Mathematical theory for the coupled atmosphere-ocean models J. Math. Pures Appl. **74** 105–163
- [42] Shapiro M A (1984) Meteorological tower measurements of a surface cold front. Mon. Weather Rev. 112, pp1634-1639.
- [43] Weaver J F and Purdom J F W (1995) An Interesting Mesoscale Storm-Environment Interaction Observed Just Prior to Changes in Severe Storm Behavior, Weather and Forecasting **10** Issue 2 449-453
- [44] Evans J S and Doswell C A III (2001) Examination of Derecho Environments Using Proximity Soundings, Weather and Forecasting **16** Issue 3 329-342
- [45] Klimowski B A, Bunkers M J, Hjelmfelt M R and Covert J N (2003) Severe Convective Windstorms over the Northern High Plains of the United States Weather and Forecasting **18** Issue 3 502-519
- [46] Klimowski B A, Hjelmfelt M R, and Bunkers M J (2004) Radar Observations of the Early Evolution of Bow Echoes Weather and Forecasting **19** Issue 4 727-734